

NAVAL POSTGRADUATE SCHOOL Monterey, California



THESIS

**BARRIER PATROL AND AIR DEFENSE SYSTEM:
DEVELOPING AND INTEGRATING FLIGHT PROFILES**

by

Luiz Alberto Pereira Bianchi

December 2002

Thesis Advisor:
Second Reader:

Steven E. Pilnick
Thomas H. Hoivik

Approved for public release; distribution is unlimited

THIS PAGE INTENTIONALLY LEFT BLANK

REPORT DOCUMENTATION PAGE			Form Approved OMB No. 0704-0188	
Public reporting burden for this collection of information is estimated to average 1 hour per response, including the time for reviewing instruction, searching existing data sources, gathering and maintaining the data needed, and completing and reviewing the collection of information. Send comments regarding this burden estimate or any other aspect of this collection of information, including suggestions for reducing this burden, to Washington headquarters Services, Directorate for Information Operations and Reports, 1215 Jefferson Davis Highway, Suite 1204, Arlington, VA 22202-4302, and to the Office of Management and Budget, Paperwork Reduction Project (0704-0188) Washington DC 20503.				
1. AGENCY USE ONLY (Leave blank)		2. REPORT DATE December 2002	3. REPORT TYPE AND DATES COVERED Master's Thesis	
4. TITLE AND SUBTITLE: Barrier Patrol and Air Defense System: Developing and Integrating Flight Profiles			5. FUNDING NUMBERS	
6. AUTHOR(S) Luiz Alberto Pereira Bianchi				
7. PERFORMING ORGANIZATION NAME(S) AND ADDRESS(ES) Naval Postgraduate School Monterey, CA 93943-5000			8. PERFORMING ORGANIZATION REPORT NUMBER	
9. SPONSORING /MONITORING AGENCY NAME(S) AND ADDRESS(ES) N/A			10. SPONSORING/MONITORING AGENCY REPORT NUMBER	
11. SUPPLEMENTARY NOTES The views expressed in this thesis are those of the author and do not reflect the official policy or position of the Department of Defense or the U.S. Government.				
12a. DISTRIBUTION / AVAILABILITY STATEMENT Approved for public release; distribution is unlimited			12b. DISTRIBUTION CODE	
13. ABSTRACT (maximum 200 words) In order to support the Brazilian Air Defense System, principally, in the Amazon region, the Brazilian Air Force has recently acquired the R-99, Airborne Warning And Control System (AWACS). This aircraft and the types of missions it can support are innovative in the Brazilian Air Force. The R-99 will be used for patrolling the Brazilian borders and interception control of illicit air traffic in the Amazon region. This thesis develops a planning tool, called the Campaign Decision Aid, to optimize the utilization of the R-99 in its search and detection mission. Basic principles of Radar Theory and simple Search and Detection models are used to support the analytical evaluation and optimal selection of the R-99 patrolling flight profiles. Also, Stochastic modeling theory is used to develop measures of effectiveness to evaluate the integrated effort of detaining the illegal traffic using interceptors, which are flown from pre-determined Air Bases in the Amazon Region. Utilization of this Campaign Decision Aid will contribute to the control and integrity of Brazilian territory.				
14. SUBJECT TERMS Air Defense, Patrolling Optimization, Measures of Effectiveness, AWACS, Air Surveillance			15. NUMBER OF PAGES 91	
			16. PRICE CODE	
17. SECURITY CLASSIFICATION OF REPORT Unclassified	18. SECURITY CLASSIFICATION OF THIS PAGE Unclassified	19. SECURITY CLASSIFICATION OF ABSTRACT Unclassified	20. LIMITATION OF ABSTRACT UL	

THIS PAGE INTENTIONALLY LEFT BLANK

Approved for public release; distribution is unlimited

**BARRIER PATROL AND AIR DEFENSE SYSTEM:
DEVELOPING AND INTEGRATING FLIGHT PROFILES**

Luiz Alberto Pereira Bianchi
Major, Brazilian Air Force
B.S., Brazilian Air Force Academy, 1985

Submitted in partial fulfillment of the
requirements for the degree of

MASTER OF SCIENCE IN OPERATIONS RESEARCH

from the

**NAVAL POSTGRADUATE SCHOOL
December 2002**

Author: Luiz Alberto Pereira Bianchi

Approved by: Steven E. Pilnick
Thesis Advisor

Thomas H. Hoivik
Second Reader

James N. Eagle
Chairman, Department of Operations Research

THIS PAGE INTENTIONALLY LEFT BLANK

ABSTRACT

In order to support the Brazilian Air Defense System, principally, in the Amazon region, the Brazilian Air Force has recently acquired the R-99, Airborne Warning and Control System (AWACS). This aircraft and the types of missions it can support are innovative in the Brazilian Air Force. The R-99 will be used for patrolling the Brazilian borders and interception control of illicit air traffic in the Amazon region. This thesis develops a planning tool, called the Campaign Decision Aid, to optimize the utilization of the R-99 in its search and detection mission. Basic principles of Radar Theory and simple Search and Detection models are used to support the analytical evaluation and optimal selection of the R-99 patrolling flight profiles. Also, Stochastic modeling theory is used to develop measures of effectiveness to evaluate the integrated effort of detaining the illegal traffic using interceptors, which are flown from pre-determined Air Bases in the Amazon Region. Utilization of this Campaign Decision Aid will contribute to the control and integrity of Brazilian territory.

THIS PAGE INTENTIONALLY LEFT BLANK

TABLE OF CONTENTS

I.	INTRODUCTION.....	1
A.	PURPOSE	1
B.	SCOPE AND METHODOLOGY	2
	1. Parameters Derivation.....	2
	2. Parameters Selection.....	2
	3. Lateral Range Development.....	2
	4. AWACS Profiles Evaluation	3
	5. Comparative Analysis.....	3
	6. Development of Interception Measures of Performance.....	3
C.	ORGANIZATION OF STUDY.....	3
II.	SCENARIO DESCRIPTION.....	5
III.	AWACS PLATFORM OVERVIEW	7
A.	TECHNICAL FEATURES	8
	1. Radar Frequency.....	8
	2. Maximum Unambiguous Detection Range	9
	3. Pulse Repetition Frequency.....	9
	4. Minimum Detection Range.....	9
	5. Maximum Detection Range	10
	6. 3-dB Beamwidth	11
	7. Horizontal Coverage	13
B.	OPERATIONAL FEATURES.....	14
	1. Flight Velocity Range.....	14
	2. Operational On Station Altitudes	14
	3. Endurance	16
B.	LATERAL RANGE FUNCTION.....	16
IV.	BARRIER PATROL PROFILES AND COMPARISONS	21
A.	ASSUMPTIONS.....	21
B.	SWEEP WIDTH.....	22
C.	SYMMETRIC LINEAR PATROL	26
	1. Search Geometry	26
	2. Results	29
D.	SYMMETRIC CROSSOVER PATROL	32
	1. Search Geometry	32
	2. Results	36
E.	PATROL PATTERN COMPARISONS	38
	1. Searcher Speed Effects.....	38
	2. Relative Speed Effects.....	38
	3. CDP Effects.....	38

4.	Searcher-Altitude Effects	38
5.	Patrol Area.....	39
6.	Optimum Search Length	39
7.	Prior Target Knowledge	40
V.	CAMPAIGN DECISION AID	41
A.	SEARCHER'S MINIMUM AVAILABILITY	42
B.	SEARCHER'S PROFILE SELECTION.....	46
C.	CAMPAIGN'S MEASURES OF EFFECTIVENESS	47
D.	SUMMARY.....	55
VI.	CONCLUSIONS AND RECOMMENDATIONS.....	57
A.	GENERAL	57
B.	CONCLUSIONS.....	59
1.	R-99 Surveillance Capabilities	59
2.	Patrolling Profiles Particularities	60
	<i>a. Searcher and Target Speed Effects.....</i>	<i>60</i>
	<i>b. Searcher Altitude Effects</i>	<i>60</i>
3.	Campaign Effectiveness.....	61
	<i>a. Interceptor Speed.....</i>	<i>61</i>
	<i>b. Interception Tactics.....</i>	<i>62</i>
	<i>c. Preset Interception Line</i>	<i>62</i>
	<i>d. Searcher's Base Relative Location</i>	<i>62</i>
C.	RECOMMENDATIONS	63
1.	Validation of the CDA.....	63
2.	Radar Performance Testing	63
3.	Areas For Future Research	63
	<i>a. R-99 Data Analysis.....</i>	<i>63</i>
	<i>b. Model Simulation</i>	<i>64</i>
	LIST OF REFERENCES	65
	INITIAL DISTRIBUTION LIST	67

THIS PAGE INTENTIONALLY LEFT BLANK

LIST OF FIGURES

Figure 1.	Patrolling Region of Interest	6
Figure 2.	Embraer 145 AEW&C	7
Figure 3.	Minimum Detection Range	10
Figure 4.	3 dB Beamwidth.....	12
Figure 5.	Vertical Silence Radar Zones.....	12
Figure 6.	Horizontal Scanning and Horizontal Blind Radar Zones.....	13
Figure 7.	Vertical Silence Zones	15
Figure 8.	Horizontal Silence Zones and Relative Detection Geometry (I).....	17
Figure 9.	Lateral Range Curve.....	18
Figure 10.	Horizontal Silence Zones and Relative Detection Geometry (II)	19
Figure 11.	Lateral Range Curve for Inner Detection Gaps.....	20
Figure 12.	Altitude's Effect on Sweep Width	23
Figure 13.	Radar Coverage Constraints.....	24
Figure 14.	Radar Coverage Graph	25
Figure 15.	Symmetric Linear Patrol	26
Figure 16.	Target-Searcher Approaching Angle Variation	27
Figure 17.	Symmetric Linear Patrol Dynamics	28
Figure 18.	Linear Profile Computations	29
Figure 19.	Linear Patrol CDPs – Searcher at 5780 ft	30
Figure 20.	Altitude Effect on Linear Profile CDP	32
Figure 21.	Symmetric Crossover Barrier Patrol Geometry	33
Figure 22.	Crossover Barrier Patrol – Cross-Angle.....	33
Figure 23.	Crossover Barrier Patrol Dynamics.....	34
Figure 24.	Crossover Profile Computations	36
Figure 25.	Effect of Altitude on Crossover CDPs	37
Figure 26.	Crossover Barrier Patrol CDPs- Searcher at 28000 ft.....	37
Figure 27.	Crossover versus linear barrier patrol.	39
Figure 28.	Optimum Search Length Comparison.....	40
Figure 29.	Campaign Decision Aid User Interface	41
Figure 30.	Air Bases Coordinates Entry	43
Figure 31.	Coordinates' Referential Description.....	43
Figure 32.	Infeasible On Station Time	44
Figure 33.	Feasible On Station Time After Adding Third Searcher.....	45
Figure 34.	Feasible On Station Time Profiles	46
Figure 35.	Required On Station Time.....	46
Figure 36.	Searcher Profile Selection	46
Figure 37.	Search Profile Summary.....	47
Figure 38.	Reaction Time Factors	48
Figure 39.	Interception Set up	50
Figure 40.	Interception Time Spreadsheet Calculations.....	51
Figure 41.	GLI Model.....	52

Figure 42.	Campaign MOPs	53
Figure 43.	Target's Flight Time To Preset Interception Line.....	55

THIS PAGE INTENTIONALLY LEFT BLANK

LIST OF TABLES

Table 1.	Target-Searcher Speed Ratio and Sweep Width Effect	28
Table 2.	Target-Speed Ratio Effects on CDP.....	31
Table 3.	Searcher Speed and Sweep Width Variation.....	34
Table 4.	Searcher's Maximum Available Flight Times (hours).....	45

THIS PAGE INTENTIONALLY LEFT BLANK

ACKNOWLEDGMENTS

I would like to express my gratitude to those who contributed to the successful and timely completion of this thesis. First I would like to thank Professor Steven E. Pilnick for his patience, guidance and constant support. I would like also to thank Professor Thomas H. Hoivik for his expertise, cooperation and outstanding willingness reading this thesis. Other members of the NPS faculty also have my appreciation for their excellent instruction.

My deepest gratitude also goes to the Brazilian Air Force, especially those who believed in my professional dedication.

Finally, I would like to thank my wife Natasha for her support and understanding as I worked on this thesis.

THIS PAGE INTENTIONALLY LEFT BLANK

EXECUTIVE SUMMARY

Recently, the Brazilian Air Force was equipped with a new Airborne Warning and Control System (AWACS), the R-99. This Brazilian made aircraft is intended to establish an effective surveillance in the Amazonian region. This region has been frequently crossed by illicit air traffic, normally related to narcotics transportation. Furthermore, this region has been the focus of recent media reports about revolutionary foreign forces trying to expand their influence across the Brazilian border. This thesis investigates R-99 employment options for maximizing mission effectiveness with limited assets. Since the area for possible illicit air traffic is extensive, this thesis develops a computerized tactical planning tool or Campaign Decision Aid (CDA) for determining optimum employment of the R-99 in these campaigns.

This Campaign Decision Aid focuses on using several R-99 aircraft to continuously patrol a limited segment of the Brazilian border for a limited number of days. This is because it is assumed that after several days of successfully patrol and interception operations by the Brazilian Air Force, the illicit traffic will decrease significantly due attrition, or shift to a different pattern in another area. At most, three consecutive days of operations are a reasonable period suitable for this kind of concentrated patrolling campaign; as a result, this CDA uses this operating period.

Two feasible patrolling geometries or profiles are analyzed: symmetric linear and symmetric crossover. Each of these profiles are separately analyzed and evaluated in terms of probability of detection, a measure of barrier patrol effectiveness. All influential parameters for each profile are listed, evaluated, and related to its specific contribution in the overall profile result. The results are then compared and the significant findings are listed below:

1. Searcher Speed Effects

In the linear patrol design, the cumulative detection probability (CDP) for a given target speed has a low variation as the searcher increases its speed. However in the crossover design, the searcher speed parameter has a stronger effect in the achieved CDP.

2. Relative Speed Effects

For a given a target speed, the linear profile achieves greater CDP from lower searcher speeds up to a point where the crossover design attains better CDP results. This fact is amplified as the targets speeds became larger. Therefore, the optimum patrol profile depends on the speeds of both, target and searcher.

3. CDP Effects

At a target speed of 150 kt, the crossover patrol is the only design that reaches a CDP equaling 1. The linear patrol pattern is unable to guarantee a target detection probability equal to 1 for the target's assumed speed.

4. Searcher-Altitude Effects

The searcher altitude negatively affect the crossover patrol geometry at flight levels above the optimal altitude (5775 ft); that is, the higher the searcher altitude, the lower the CDP. On the other hand, different searcher's altitudes do not affect the linear patrol geometry's CDP.

5. Patrol Area

The portion of space necessary to apply both geometries is also an important aspect to be considered. The linear patrol always requires the same area to be employed. On the other hand, the crossover pattern varies with area limits for each target-searcher combination. The area length is the same for both profiles, but crossover profile is wider than linear design for target speeds greater than 0 kt.

6. Optimum Search Length

The optimum search length is where the respective patrol design achieves CDP equals 1. The linear patrol geometry covers larger optimal search lengths than the crossover patrol design. Additionally, lower target speeds resulted in bigger optimal search lengths.

7. Prior Target Knowledge

The linear design does not depend on previous knowledge of target speed, because the searcher always performs the same path (back and fourth). In contrast, the crossover pattern is set based on previous target speed information. A good target speed estimate can provide a better geometry and more reliable results, but inaccurate target knowledge can cause under or over estimations of CDP.

This initial methodology only evaluates the R-99 surveillance capability for different patrolling profiles. In order to integrate the R-99 detection capabilities and target interception task, Air Base locations and their influence in terms of search time availability (on station time) are analyzed in relation to the patrolling profiles. Stochastic models theory is used to evaluate the effectiveness of this integrated effort. The CDA measures the campaign effectiveness in terms of number of targets intercepted during the operation. The result depends on various factors such as

- The number of available Air Bases as well as their relative position to the searched area
- The searched area's length, the interceptors' speed, the position where the target is detected
- The patrolling profile, the preset interception line, the interception tactics: ground launch interception (GLI) or combat air patrol (CAP)
- The inter-arrival time of targets
- The target speed

As observed, the variables involved in this measurement are numerous. Some of these variables may assume a wide range of possibilities, such as interceptor speed or interception tactics. Other variables may not, as in the case of the Base's location and area searched. Therefore, each case has to be evaluated for the intended campaign and their respective particularities. Nonetheless, some conclusions are identified through this thesis and are enumerated in the following paragraphs.

1. Interceptor Speed

The faster the interceptor, the higher the number of detected targets and the higher the percentage of targets intercepted. This comment is applicable to both interceptor procedures (GLI or CAP); however, the effects are more evident when GLI is the chosen tactic.

2. Interception Tactics

The combat air patrol (CAP) interception is always better than the ground launch interception (GLI) since the measure of effectiveness (MOE) results in better outcomes. That is, the expected number of targets lost is smaller, the number of targets detected is higher, and the number of targets capable of being intercepted is higher during campaign. However, the logistic support as well as the personnel required to maintain a CAP station during an entire campaign has to be evaluated and compared to the means available for the operation.

3. Preset Interception Line

Moving the preset interception line far from the border increases the target flight time more than the interceptor flight time to this line, since the interceptor speed is assumed to be higher than target speed. Therefore the farther the preset interception line is from the border, the higher is the percentage of targets that can be intercepted.

4. Searcher's Base Relative Location

Base location is an important aspect to be considered in the campaign planning. This is because the time spent in transit to and from the search area takes away from the available time on station. As a consequence, for a fixed number of aircraft, a base at great distance from the search area restricts the flight profiles (altitudes and speeds) available on station and negatively affects the CDP. Furthermore, some bases' location may be completely restrictive in terms of mission continuity so that the number of searchers has to be increased in order to avoid search interruption. Therefore, the closer the base is to the search area, the more flexible the profile selection and required number of needed searchers is for an uninterrupted campaign.

The computerized Campaign Decision Aid incorporates all influential parameters investigated in this thesis. Although a many variables need to be considered for measures of effectiveness evaluation, the CDA provides immediate response to any desired campaign set up. Additionally, the CDA is very flexible regarding new input data. Radar parameters, R-99 operational data, target altitudes, Air Bases locations, interceptor types are easily changed by the user. As a result, the CDA can also be a useful tool in planning missions for other AWACS (Airborne Warning and Control System) aircraft in different regions. The CDA can be readily used to obtain an immediate evaluation of the potential campaign's effectiveness for the different tactical factors. Finally, because the CDA is specific about numbers and basing of AWACS and interceptors, the CDA can be used to assess campaign cost and manpower requirements for the overall operation.

THIS PAGE INTENTIONALLY LEFT BLANK

I. INTRODUCTION

Territory integrity protection and control are the primary tasks of the Brazilian Armed Force. Electronic devices are crucial in accomplishing such jobs when the area dimensions and topography exceed human capabilities.

Searching for an efficient way to contribute to such an important mission, the Brazilian Air Force has been equipped with a new Airborne and Control System (AWACS) to control the air space in regions where the conventional ground based radar is restricted in range by natural obstacles. The recently new Brazilian made aircraft is intended to be employed initially in the Amazon region, where the sparse population and the dense forest demand a more sophisticated way of control.

The operation of this asset, AWACS, is focused in one of the most important regions of Brazilian territory, the Amazonian Forest, which has a global importance because of its rich natural resources and the increasing illicit air traffic, normally related to narcotics transportation. Furthermore, recent media reports indicate that revolutionary foreign forces are trying to expand their influence across the Brazilian border.

All these facts arouse the need for efficient surveillance over this region to prevent illegal activities. Since the means of surveillance are limited due to the extensive area of interest, the employment of AWACS aircraft has to be optimized.

A. PURPOSE

The purpose of this thesis is to develop a tactical planning tool able to generate optimal employment methods for utilizing AWACS aircraft in campaigns and scenarios against illicit air traffic.

Operational employment alternatives of this complex and valuable platform are developed, analyzed and evaluated using commonly available data from unclassified publications and using Search and Detection and Radar Theories.

Several variables are explored and evaluated to enable developing complete flight profiles. Flight altitude is one of the crucial aspects because it reflects directly on the

availability of time for the mission, on the radar horizon, on the lateral range function, on the cumulative probability of detecting particular sensor-target geometries and on radar theory. Other important analyzed variables are velocity, flight paths and leg lengths.

All variables analyzed must encounter a trade off between detection capabilities and interception control in order to close the air defense cycle. Because of that, interceptor base locations relative to the AWACS flight position must be considered when analyzing its effort on the other flight variables to ensure air defense cycle efficiency.

This thesis additionally evaluates the number of platform required in the campaign in order to achieve an uninterrupted control of the designated patrolling. Scenarios are evaluated in terms of assets utilized and operation days.

B. SCOPE AND METHODOLOGY

This thesis examines the use of the AWACS in a barrier patrol mission by comparing, analyzing and evaluating various AWACS technical details (flight and radar parameters). A sensitivity analysis will be conducted on the variables to optimize sensor capability and develop suitable mission flight profiles.

The methodology used in this thesis research consists of the following steps:

1. Parameters Derivation

Radar theory is used to generate suitable technical parameters to support this research. Many necessary data are of a confidential nature and others still need to be tested and evaluated to check the information presented in technical orders.

2. Parameters Selection

Analyze and make a selection of radar parameters that contribute directly to the AWACS coverage area.

3. Lateral Range Development

Develop considerations and set up Lateral Range Function related to AWACS radar.

4. AWACS Profiles Evaluation

Develop methods to evaluate two chosen AWACS patrolling tracks (linear and crossover profiles) and their resulting cumulative probability of detection.

5. Comparative Analysis

Conduct a comparative analysis and effectiveness evaluation for selected flight parameters.

6. Development of Interception Measures of Performance

Evaluate the interception geometry (Ground Launch Interceptors or Combat Air Patrol) for a specific scenario involving the AWACS platform and interceptors.

C. ORGANIZATION OF STUDY

The study commences with Chapter II describing the applicable operational scenario. Chapter III presents the AWACS features and investigates some tactical and technical details of that aircraft. This provides a more thorough background about the operation particularities of such a platform allowing selection of parameters (flight and radar settings) related directly to the results of a barrier patrol. Besides that, this chapter presents the development of the lateral range function.

Chapter IV describes the development of the sensor sweep width, which directly affects the cumulative probability of detection. After that explanation, the two elected patrol designs are presented, analyzed, evaluated and compared in terms of flight profiles and the resulting cumulative detection probability.

Chapter V describes how the campaign planning tool, designated as Campaign Decision Aid (CDA), integrates mission influential factors and the sensitivity analysis previously established in Chapter IV. The method adopted to produce campaign's measures of effectiveness presented in CDA is also described.

Chapter VI summarizes all others chapters and gives a straight sight of the main steps followed to achieve the final product of this thesis: the Campaign Decision Aid. Furthermore, this chapter presents conclusions and recommendations for future research.

THIS PAGE INTENTIONALLY LEFT BLANK

II. SCENARIO DESCRIPTION

As addressed in the introduction, the illegal incursion in the Brazilian territory is one of the priority objectives as soon as the AWACS operationally employed.

This thesis focuses on using the AWACS in limited space and time, because routine patrolling will not obtain continuous positive results. This is due to the opponent's awareness that such an operation can in some how interfere with the randomness of the traffic across the borders. A limited but intense campaign is a key improvement factor that surprises the opponent during patrolling. Since the means of the communication network are amply utilized by illegal organizations, as soon as the first actions are implemented, the intensity of the traffic will be reduced drastically. Therefore, a prolonged operation gains no benefits when compared to concentrated operations. At most, three consecutive days of operations are a reasonable period suitable for this kind of concentrated patrolling campaign; as a result, this thesis assumes this period of operation.

The region to be searched is another important factor to be established at the beginning of this thesis since it directly affects patrolling efficiency, which will be shown in the following chapters. In view of the fact that operations on the borders represent an international issue and that the agreements become more difficult as the number of participants grows, the operation is placed in a region covering the borders between only two nations. Since the flight path is completely over Brazilian territory, no authorization is needed by an external organization in performing such an operation. The nature of this action is not focused against any government, but the targets can be seen as a common enemy among the countries of interest. The intended campaign is set over the entire range between Brazilian-Colombian border, which is of current interest. This definition is necessary to limit the length of the path to be covered by the searcher aircraft in the analytical equations. The Figure 2.1 identifies the region of interest and the possible air bases for the interceptor aircraft and searcher aircraft.



Figure 1. Patrolling Region of Interest

It is assumed that the course chosen by the illegal aircraft is perpendicular to the limit line between the two countries. This assumption is not far from reality because it seems that this is the safest way to cross the border without being detected by the Army platoons positioned along that line. This course should provide a minimum exposure time over the limit area.

Based on data furnished and divulged by the media, the approximated number of illicit aircraft crossing the Brazilian-Colombian border is about 60 per month and that are composed basically by small airplanes which have a cruising velocity about 150 knots. Looking for a terrain screening, these aircraft normally fly at very low altitudes varying from 500 ft to 1500 ft depending on the existence of Army platoons or small villages near the flight paths. The landing points are generally small-unpaved runways located near river banks or side roads, where the illegal merchandise is then reshipped in boats or cars for other points inside Brazilian area.

III. AWACS PLATFORM OVERVIEW

The Embraer 145 (EMB-145) Airborne Early Warning and Control (AEW&C), the aircraft considered as AWACS in this research and shown in Figure 2, is a derivative of the Embraer ERJ-145 regional jetliner airframe, modified with the integration of an Airborne Early Warning radar and mission system. The aircraft's mission system is developed around the Ericsson ERIEYE active, phased-array pulse-Doppler radar and is integrated with an onboard command and control system. Electronic surveillance measures for monitoring communication and non-communication activities are also integrated with the system.



Figure 2. Embraer 145 AEW&C

The manufacturer states that a fleet of three aircraft is sufficient to sustain two airborne patrols around the clock for a limited time, or one airborne patrol with one aircraft on continuous ground alert for more than 30 days. Information in regards to the types of patrol has not been included by the manufacture neither the specification for the term “limited time” for patrolling around the clock.

Ericsson Microwave Systems developed the ERIEYE. The system comprised of an active phased-array pulse-Doppler radar including integrated secondary surveillance radar and identification friend or foe (SSR/IFF); a comprehensive, modular command-and-control system, electronic support measures (ESM), communications and data links.

Rather than a conventional rotodome antenna system, the ERIEYE has a fixed, dual-sided and electronically scanned antenna mounted on top of the fuselage. This kind of structure requires much less demand on aircraft size and is designed for mounting on commuter-type aircraft. Another specification announced by the manufacturer is that

ERIEYE is capable of 360-degree detection and tracking of air and sea. This specific capability will be examined more thoroughly later in this thesis since a dual sided antenna such as the ERIEYE has some radar coverage restrictions, which are important constraints to search efficiency. The system uses advanced solid-state electronics, open-system architecture and ruggedized commercial off-the-shelf (COTS) hardware, including general-purpose programmable workstations and full-color LCD displays. The ERIEYE radar is already in service with the Swedish Air Force and is in series production for Brazil and other customers.

This new-generation system is suitable for installing in a variety of commercial and military aircraft, including regional jet or turboprop airliners. The system meets full AEW&C requirements of detecting and tracking targets at ranges of up to 450 km over land or water.

A. TECHNICAL FEATURES

The technical parameters of interest for the mission analysis are presented in the following paragraphs. Most of the parameters detailed here, refer to the radar features and have a direct relationship to the maximum and minimum detection range, which dictates the surveillance efficiency. Some of the system performance data needed for the analysis in this thesis is not readily available from unclassified open sources. Where this is the case, this thesis takes available data and uses radar theory to develop the information necessary for further analysis.

1. Radar Frequency

The Erieye operates in the S-band (2-4 GHz) [7]. For purposes of further computations, the middle frequency range value, 3 GHz, has been selected as typical our operation frequency. The relationship among velocity of propagation (c), frequency (f) and wavelength (λ) is presented in equation 3.1[1]. Assuming $c = 3 \times 10^8$ m/s and $f = 3$ GHz, the resulting wavelength is 10 cm.

$$c = \lambda \times f \tag{3.1}$$

2. Maximum Unambiguous Detection Range

The maximum unambiguous detection range (R_u) will be assumed as 240 nm (450 Km), since that matches with the information available in the manufacturer's literature [5] and it is a usual value for this type of radar [1].

3. Pulse Repetition Frequency

The ERIEYE pulse-Doppler radar operates in a medium pulse repetition frequency (PRF) range [8] when the target of interest is an aircraft. Since the maximum unambiguous detection range is known, the expected PRF value of this radar is obtained using the following equation [7]:

$$R_u = \frac{c}{PRF \times 2} \quad (3.2)$$

Since the pulse velocity of propagation (c) is approximately $3 \times 10^8 \text{ m/s}$ and R_u is 240 nm, then the PRF is about 341 Hz.

4. Minimum Detection Range

The minimum detection range (R_{min}) will be assumed as 10 nm. This value corresponds to a radius around the radar. This parameter is directly related to the pulse width, which by turn is proportional to the maximum detection range [1]. If the focus is the ground projected (horizontal) minimum detection distance from the aircraft, denominated in this thesis as minimum horizontal detection range ($R_{min,h}$), the depressed propagation angle (α), which is half of vertical beam width radar aperture (θ_e), defined in subtitle 6, and the aircraft altitude (H) have to be considered. The equation that represents that relationship is the following:

$$R_{min,hor} = \max \left\{ \frac{H}{\tan \alpha}, \sqrt{R_{min}^2 - H^2} \right\} \quad (3.3)$$

The picture below illustrates the relationship among parameters mentioned in preceding paragraph.

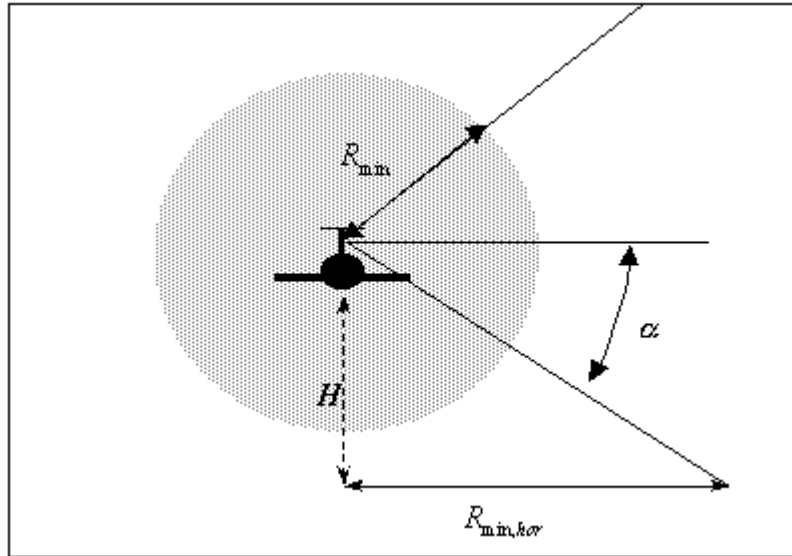


Figure 3. Minimum Detection Range

5. Maximum Detection Range

Maximum detection range (R_{max}) is one of most important parameters of this thesis since it depends on many other specific features of the radar, which are put together in the radar equation [1]. As a result, many inferences are possible as the parameters presented in such a formula are varied. Another important point is the fact that antennas such as the ERIEYE system fluctuates in power as the radar main beam is steered far from the perpendicular line to the antenna surface. This means that the detection of a target at the same flight level and across the airborne warning and control system (AWACS) is more likely to happen than any other target position [8]. Since the primary purpose is to look for targets at low altitudes, that is, below the AWACS flight level, a lower detection range due to antenna loss propagation must be taken into account when only one value is used for all 360° around the aircraft.

Besides those considerations, some physical target characteristics must be assumed. This is necessary to get the suitable target radar cross-section (RCS). Because targets are assumed to consist of small aircraft and they are not maneuverable along their flight path, a $2 m^2$ without any variation (fluctuation) is the value selected as the RCS value [7].

Ericson information [5] indicates that the maximum detection range for a target whose RCS is 2m^2 . However, data is based on an optimal detection situation, which is not the case for this thesis purposes as explained in the previous paragraphs.

As a result of the previous comments, a reduction in this parameter is necessary in order to guarantee, or at least, assume a positive detection at the assumed range. Therefore, the maximum detection range (R_{max}) is considered 120 nm. Since this parameter plays an important role in patrolling mission efficiency, a better and more reliable value to this parameter will be obtained from operational testing since there is not much detailed information available about this parameter at this time.

6. 3-dB Beamwidth

The 3 dB beamwidth or half power beamwidth is the angular separation between the half power points on the antenna radiation pattern, where the gain is one half the maximum value [11].

As observed in the Figure 4, there is a small radiation portion outside of 3 dB. Conversely, there is a region with no radiation between the main lobe and 3 dB angle. Because of that and to simplify further considerations, the 3 dB angle is assumed as a standard to represent the nominal radar propagation zone in this thesis.

The vertical 3 dB angle is fundamental to define the radar vertical coverage area, which determines the vertical blind zones below and above the AWACS. As the targets are assumed to fly at altitudes lower than the AWACS, only the blind zone below the surveillance aircraft is of interest in this thesis. Since θ_e is constant and the vertical scanning is assumed as a not available feature in this radar, as the platform varies the altitude (H), the blind portion will also change. That fact questions whether the AWACS flight level will interfere in the patrolling efficiency. This question, however, will be answered later when the overall platform patrolling efficiency is analyzed.

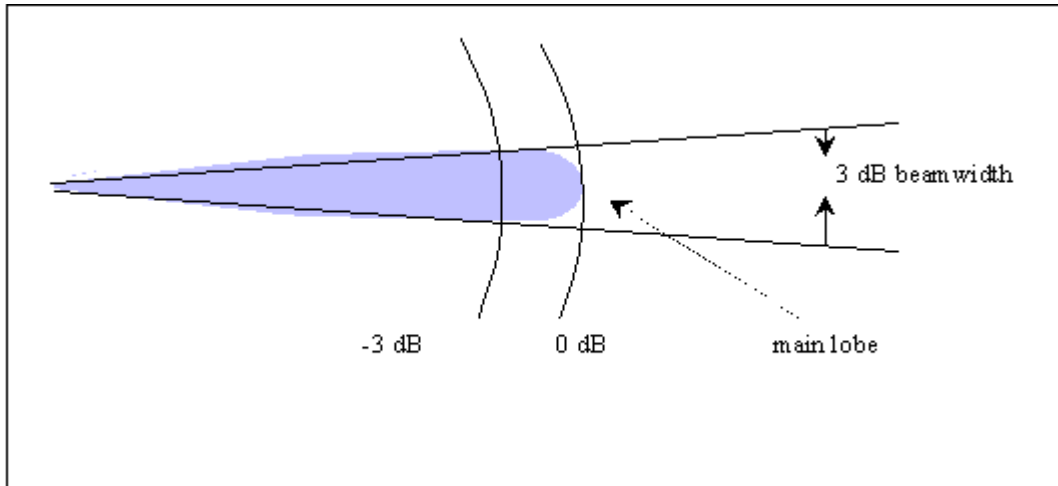


Figure 4. 3 dB Beamwidth

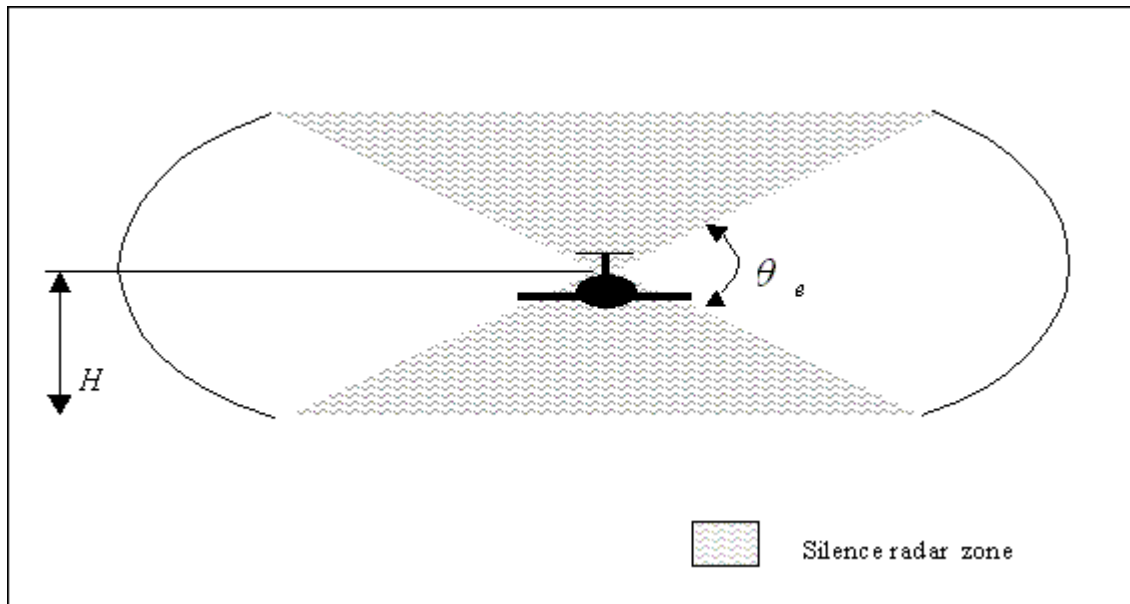


Figure 5. Vertical Silence Radar Zones

The Equation 3.4 [7] establishes the relationship between θ_e , wavelength and the antenna vertical dimensions (D) [9]. Setting these later parameters, θ_e value results in 10° .

$$\theta_e = 70 \frac{\lambda}{D} \text{ (degrees)} \quad (3.4)$$

The Figure 5 shows the vertical radar coverage limitation, which is dictated by the 3-dB beamwidth aperture angle. As seen in the picture, the vertical silence radar becomes smaller as the aperture angle increases. The only way to get smaller silence zones, in this specific case, is decreasing the flight altitude (H), which holds the relation to the minimum horizontal detection range as showed in the Equation 3.3.

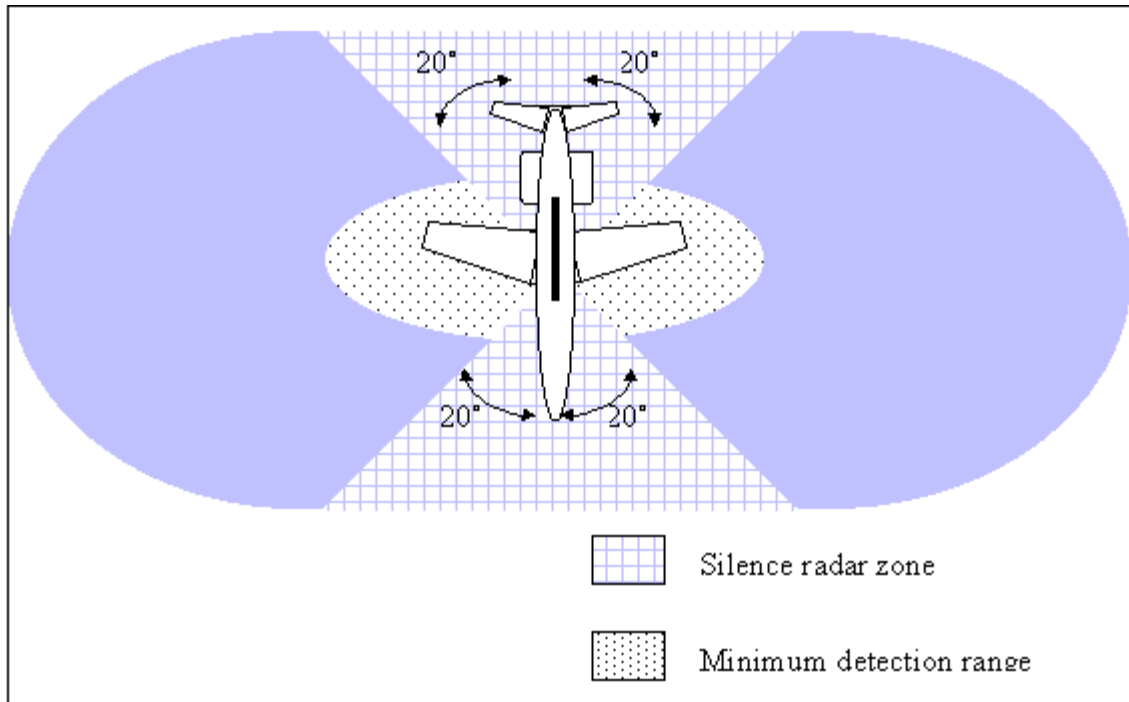


Figure 6. Horizontal Scanning and Horizontal Blind Radar Zones

7. Horizontal Coverage

Defining horizontal coverage is essential in this study because at the beginning of this chapter the manufacturer's data only presented a general platform overview for commercial purposes. Therefore, this parameter must be refined to obtain a more reliable technical data for this particular radar capability. Ericson states that a 360° coverage is accomplished for this radar, but, in fact, that type of antenna is unable to complete a circular scanning [8]. Actually, the effective antenna steering is assumed as $\pm 70^\circ$ from the perpendicular antenna surface as seen in Figure 6. The remaining uncovered area is

called silence radar zone and computerized assets automatically track the targets previously detected as they enter this region.

B. OPERATIONAL FEATURES

1. Flight Velocity Range

The Embraer 145 AEW&C has an operational velocity range that goes from 140 kt to 340 kt [5]. This flight aircraft attribute is an important aspect to be discussed in future chapters because there is a direct relationship between that parameter and cumulative detection probability, as explained later.

2. Operational On Station Altitudes

Operational on station altitudes interferes directly on the aircraft's operational employment as well as on its radar capabilities. The operational employment is affected because the endurance is inversely proportional to the flight altitude. Due to this relationship, the time available on station is directly affected. This dictates the need for repositioning intervals to complete the overall campaign duration.

As previously mentioned, the altitude also determines the silence radar area below the platform, which has a triangle format as showed in the Figure 5. Actuality, the half-length triangle base value ($R_{min,hor}$) is the measure of interest, since the objective is to detect targets flying near the ground. Using equation 3.3 and setting the corresponding values for α^1 and R_{min}^2 , the smaller $R_{min,hor}$ values are obtained as descending from the highest flight level towards the ground. Upon reaching the altitude of 5296 ft, the smallest $R_{min,hor}$ is set as 9.96 nm. If we descend more than this altitude, $R_{min,hor}$ is constrained by the minimum detection range (R_{min}), which was assumed as 10 nm. For that reason, no advantage exists in flying below that altitude when trying to decrease

¹ $\alpha = \theta_e/2 = 5^\circ$

² R_{min} is assumed as 10 nm

$R_{min,hor}$. Besides that, lower altitudes increase fuel consumption and decrease the horizon radar range as explained in next paragraph.

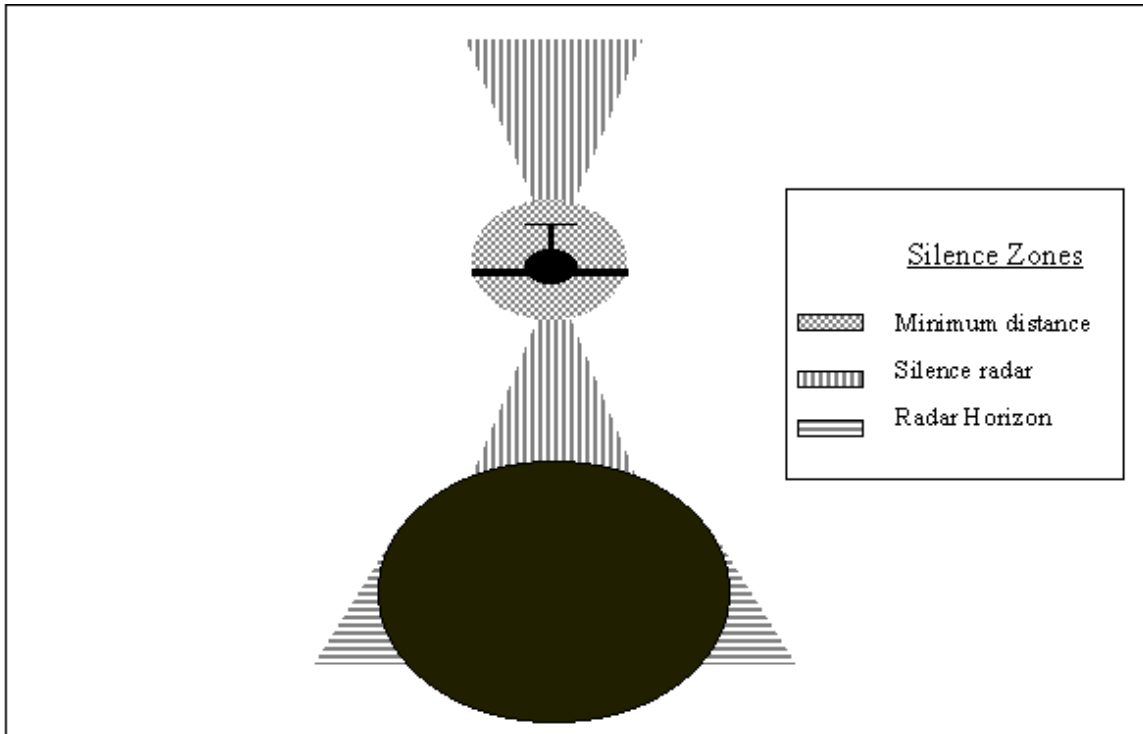


Figure 7. Vertical Silence Zones

Another significant parameter dictated by the searcher altitude is the radar horizon range R_{hor} . The Equation 3.5 [10] gives the radar horizon range in nautical miles for an antenna height (H), in this case platform altitude, set in feet. Since targets are also aircraft, that is, they might be at different altitudes, we have to set that formula twice and add both values in order to get the resulting horizon radar range. As discussed in the scenario description chapter, the targets of interest are those with flight altitudes low enough to deny the ground based radar detection. Therefore, a target altitude (h) of 500 ft (worst situation) is assumed. Setting $R_{hor}=120\text{nm}$ as the maximum detection range value, the minimum altitude for full radar detection range capability, is equal to 5775 ft.

$$R_{hor} = 1.22\sqrt{h} + 1.22\sqrt{H} \quad (3.5)$$

The last paragraphs explain the influence of altitude over the vertical radar blind zones, illustrated in Figure 7. As noticed, a conflict exists between the two previous approaches, because to make the vertical silence radar small, the radar horizon range is decreased. However, when discussing the lateral range function, this paradox becomes secondary because other parameters will prevail in terms of cumulative probability of detection depending on the patrolling geometry profile.

3. Endurance

Defined as the total flight time, the AWACS endurance is a function of flight altitude and speed. In Chapter V, more detailed considerations are presented about this parameter and its effects in the overall campaign.

B. LATERAL RANGE FUNCTION

Defined as the conditional cumulative probability of detection [6], the lateral range function $p_{(l)}(x)$ is the initial aspect to be considered when analyzing a target search accomplished by a barrier patrol. The $p_{(l)}(x)$ is a value based on the relative distances of a target that passes through the sensor detection zone. This implies in a different $p_{(l)}(x)$ depending on the relative positioning between both searcher and target since the sensor analyzed here does not have a complete radar circular coverage.

Calling the target vector \vec{u} and the searcher vector \vec{v} , the relative vector \vec{s} is the difference of the first two vectors. The vector \vec{s} represents the target relative movement to the searcher. The angle between \vec{v} and $-\vec{s}$, designated as γ , is the parameter to be observed when setting the appropriate lateral range function to the respective situation. As illustrated in Figure 8, if γ is equal or greater than ϕ , the horizontal silence radar angle, the target will always pass through the sensor detection zone.

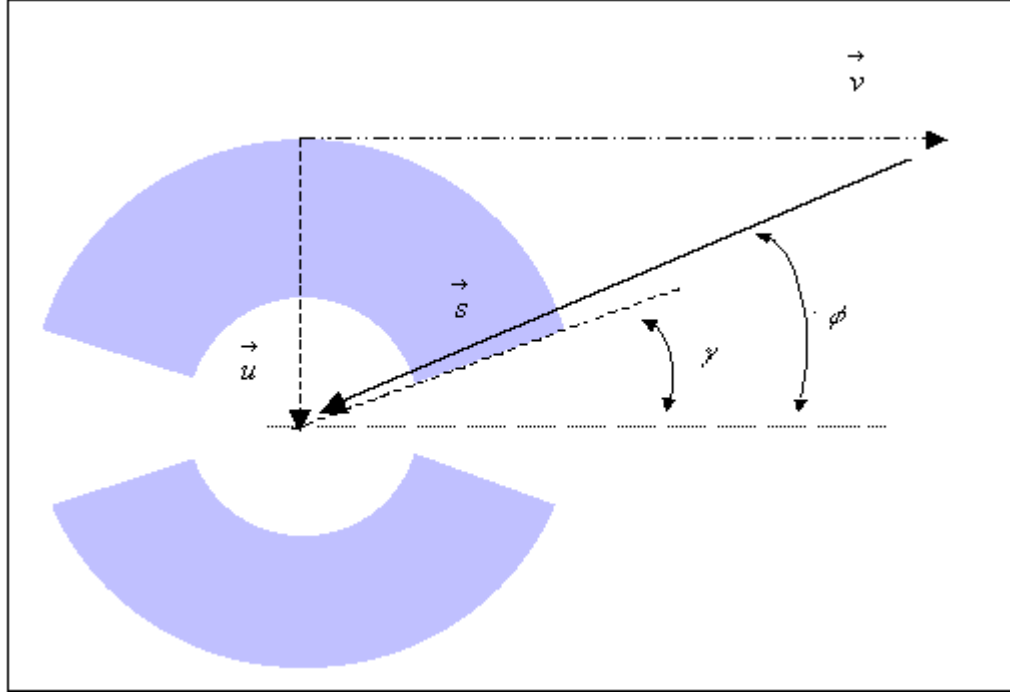


Figure 8. Horizontal Silence Zones and Relative Detection Geometry (I)

This is considered a cookie-cutter sensor since every time a target is inside the sensor detection zone the probability of detection is equal to 1. The lateral range function $p_{(l)}(x)$ for the situation illustrated in Figure 8, is that presented in Equation 3.6. The term $R_{max,opr}$ represents the radar maximum operational detection range, which will be the minimum value between the radar maximum detection range (R_{max}) and the radar horizon R_{hor} (Equation 3.7).

$$p_{(l)}(x) \begin{cases} 1, & \text{when } |x| \leq R_{max,opr} \\ 0, & \text{otherwise} \end{cases} \quad (3.6)$$

$$\text{where, } R_{max,opr} = \min \{R_{max}, R_{hor}\} \quad (3.7)$$

The corresponding lateral range curve for this is shown in Figure 9.

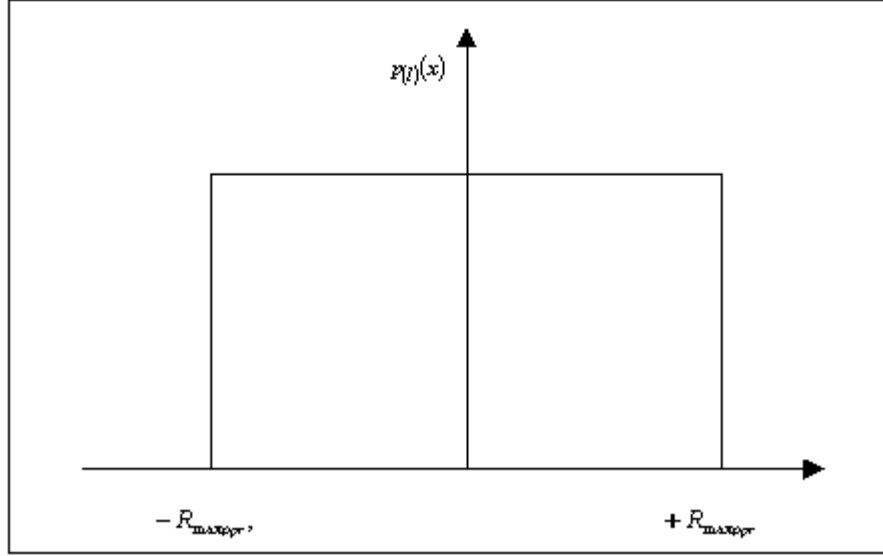


Figure 9. Lateral Range Curve

On the other hand, if γ is smaller than ϕ , shown in the Figure 10, an inner detection gap occurs. For this situation, $p_{(l)}(x)$ is conditioned to the resulting difference between γ and ϕ and is calculated using the Equation 3.8. The CPA_{null} parameter in that formula is the perpendicular distance from the radar antenna to \vec{s} . This represents the lateral inner distance value without detection due to the minimum horizontal detection range $R_{min,hor}$ and horizontal scanning limitations, as expressed in Equation 3.9. Observing the latest equation, the influence of the crossing angle, CPA_{null} is a function of $R_{min,hor}$, which has greater values as the altitude increases. On the other hand, $R_{max,opr}$ has a contrary behavior. To solve this dilemma, an optimization technique will be presented in the next chapter.

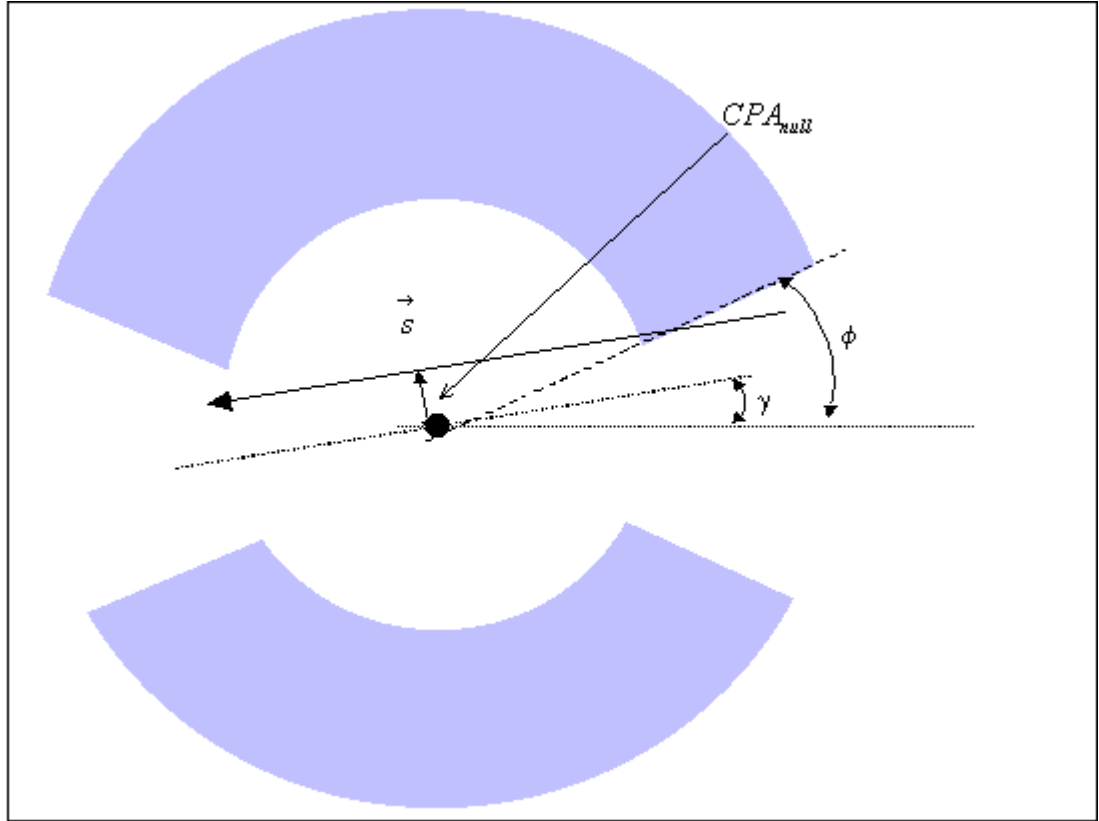


Figure 10. Horizontal Silence Zones and Relative Detection Geometry (II)

$$p_{(t)}(x) \begin{cases} 1, & \text{when } CPA_{null} |x| \leq R_{max,opr} \\ 0, & \text{otherwise} \end{cases} \quad (3.8)$$

$$\text{where, } CPA_{null} = \sin(\phi - \gamma) \times R_{min,hor} \quad (3.9)$$

The corresponding lateral range curve for that case is shown in Figure 11.

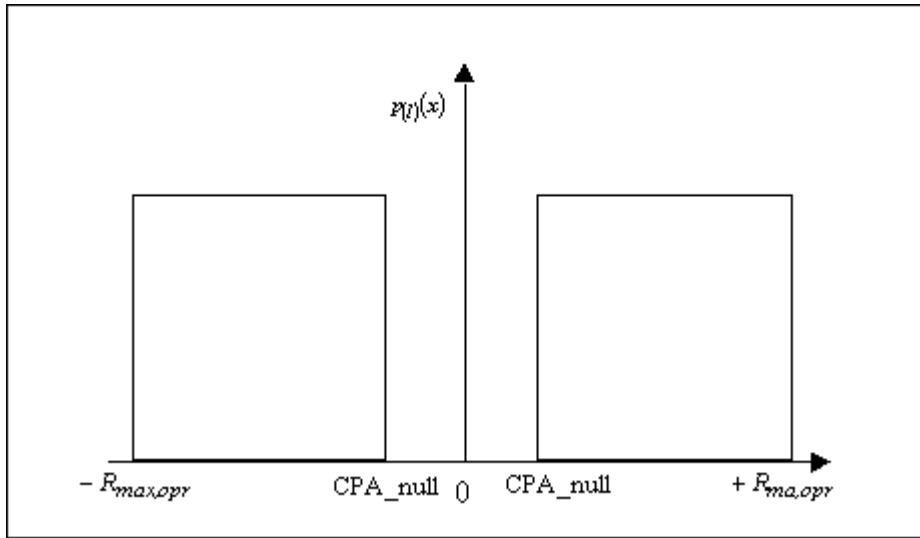


Figure 11. Lateral Range Curve for Inner Detection Gaps

Based on the discussion presented in this chapter, we have conditions to start the patrolling profile investigation in the next chapter.

IV. BARRIER PATROL PROFILES AND COMPARISONS

This chapter introduces the two selected patrolling profiles for the intended campaign against illicit traffic: linear and crossover. Both profiles are detailed in terms of geometry and the influential parameters related to each profile are analyzed and used to compare the patrolling effectiveness. Before the presentation of such a profiles, some assumptions are required as well as the introduction of a fundamental concept of Search and Detection Theory: sweep width.

A. ASSUMPTIONS

The model used to support the considerations about the cumulative detection probability requires some assumptions in order to achieve reliable results. Basically, the proposed operational scenario described in Chapter II was assembled on those model assumptions. The following is a list of important operational scenario functions used in the analytical comparisons:

- It is assumed that a target is intending to traverse a region adjacent to the border between two countries.
- The width between the stationary search extreme points, illustrated in Figure 1 (Chapter I), measures 500 nm. It is assumed the target's crossing points are uniformly distributed and always perpendicular to the imaginary line that connects the extreme points.
- The target's speed is constant along its path. This assumption is not far from reality because, after reaching the cruise level, the target aircraft usually maintains a steady speed.
- The target heading is the same from the border crossing point until the intended destination, which, in practice, represents the shortest path and the least time exposed to searcher. This may be a likely tactic employed by an illicit traffic.

The lateral range function and all calculations are based on the premise that the radar's target detection effectiveness remains unchanged during the search.

Finally, the cumulative detection probability (CDP) during a search profile is based on a Search and Detection principle. That states that CDP is the ratio between the swept area and the area of all possible points a target can pass through during the search corresponding period. As a result, the R-99 radar sweep width (w) considerations are necessary before the search patterns analysis itself.

B. SWEEP WIDTH

The radar sweep width needs to be known before of a search profile can be determined. This radar sweep width is defined by following the Equation 4.1 [10].

$$w = \int_{-R_{max,opr}}^{+R_{max,opr}} p_l(x) dx \quad (4.1)$$

Since the swept area is directly proportional to w , the appropriated lateral range function ($p_l(x)$) has to be maximized in order to achieve the biggest CDP. Therefore, the relative target-searcher approximation angle (γ) and the silence radar angle (ϕ) are the first points to be considered before any other variable in the sensitivity analysis. When γ is smaller than ϕ , the searcher altitude becomes one of the determinant variables in the search effectiveness since altitude affects w in this case. The Figure 12 illustrates the altitude's effect on sweep width when this situation occurs; that is, γ is 0° and ϕ is 20° . Because of that, some considerations are made necessary to understand that relationship.

Let the minimum operational detection range ($R_{min,opr}$) be equal the minimum horizontal detection range $R_{min,hor}$.

$$R_{min,opr} = R_{min,hor} \quad (4.2)$$

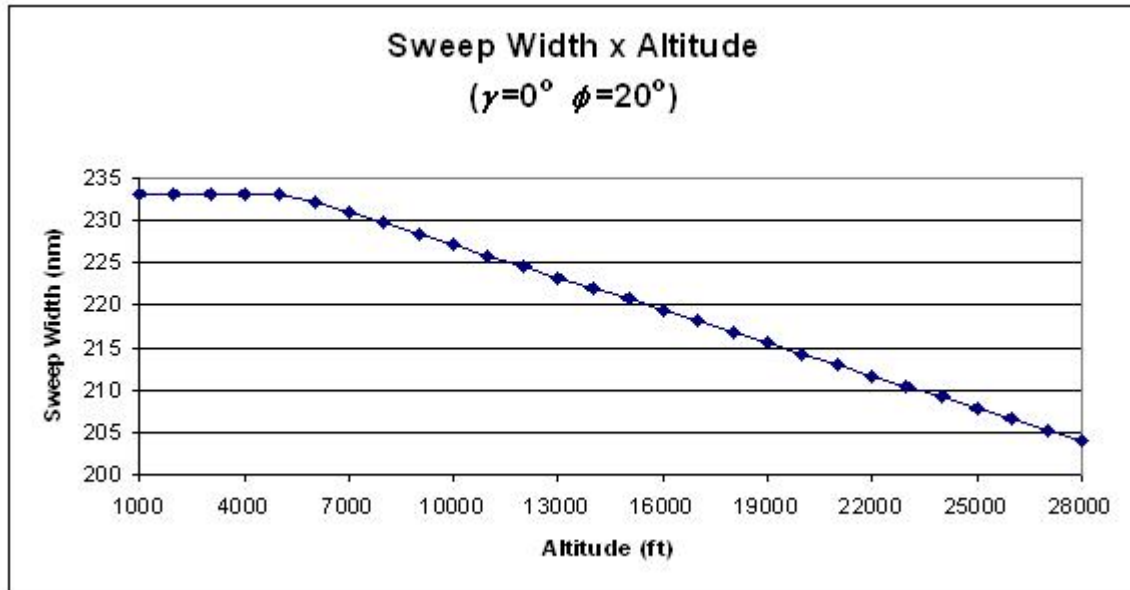


Figure 12. Altitude’s Effect on Sweep Width

Let the maximum operational detection range ($R_{max,opr}$) be the minimum value between radar maximum detection range (R_{max}) and radar horizon (R_{hor}), as defined in Equation 3.7.

The radar coverage at a specific target flight level is the difference between $R_{max,opr}$ and $R_{min,opr}$ for that level. The plot of both parameters, considering a target at 500 ft, and the respective platform altitudes is illustrated in Figure 13.

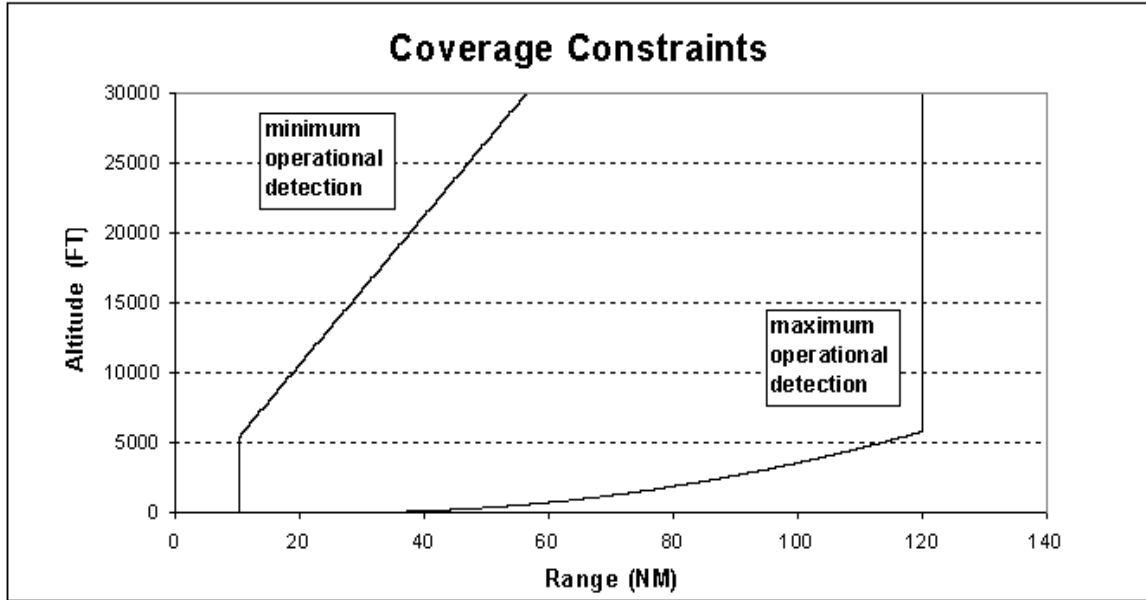


Figure 13. Radar Coverage Constraints

The coverage ranges for each platform flight level are those between the two constraint lines. To find the altitude where the largest difference between those lines exists or, to obtain the optimum coverage altitude, the following formulation applies:

$$\max_H R_{max,opr} - R_{min,opr} \tag{4.3}$$

$$\text{Subject to } \left\{ \begin{array}{l} R_{min} \geq 10 \text{ nm} \\ R_{max} \leq 120 \text{ nm} \end{array} \right\}$$

The solution of such calculations will result in the best combination of maximum operational detection range ($R_{max,opr}$) and lateral inner distance value (CPA_{null}). As a consequence, the greater sweep width is achieved. The plot of coverage ranges and respective searcher altitudes is shown in Figure 14. As the searcher altitude increases,

starting from the ground level, the coverage ranges attain bigger values. This fact is caused by a faster increase of R_{hor} than $R_{min,hor}$. At the altitude where the radar horizon reaches a value equal to the maximum detection range, further increments only increase $R_{min,hor}$, causing detection range loss. That altitude is the one that satisfies the optimization stated in Equation 4.3, for a target maintaining 500 ft of altitude.

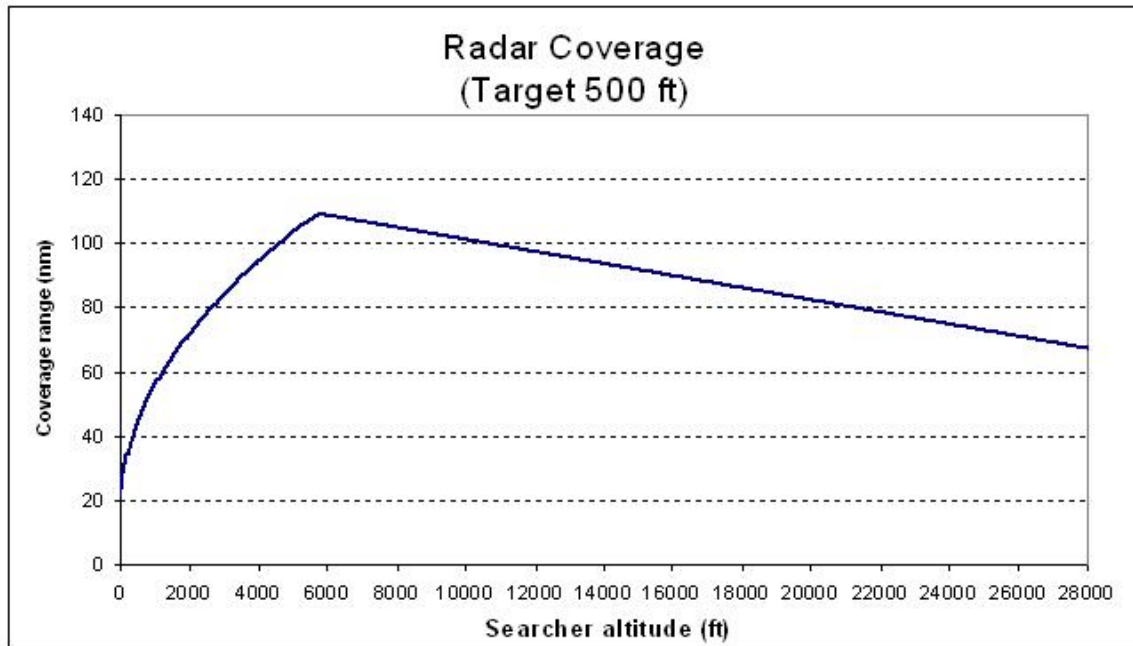


Figure 14. Radar Coverage Graph

Knowing variables implications in the searcher detection capability, the analysis can proceed in more detail to the central point of investigation: the patrolling profiles.

Instead of analyzing many different search patterns, only two of them have been chosen because, first, they are operationally feasible and, second, neither pattern relies on many changes of direction, what is a complicating technical factor for this type of platform. The more stable the AWACS, the more effective is the detection capability, so the assumption of a constant detection probability is better observed in these two cases, described below. Furthermore, the calculations, which follow, are free of the complexity of flight parameters.

C. SYMMETRIC LINEAR PATROL

1. Search Geometry

This patrol design (Figure 15) is characterized by a searcher traveling with velocity \vec{v} in a straight line back and forth movements along the border between two fixed points (A and B).

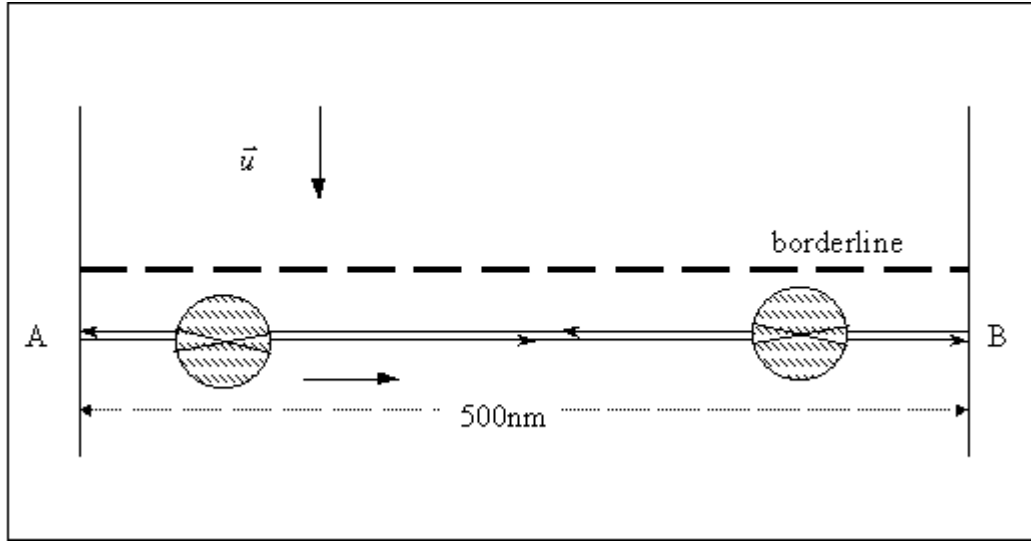


Figure 15. Symmetric Linear Patrol

A search cycle is completed each time the platforms reach the initial point, or other assumed as the starting point, consecutively. The distance between points A and B is defined as d and represents the border length. The target travels with velocity \vec{u} perpendicular to \vec{v} . The searcher executes a back turn at a distance of half sensor's searcher seep width (w) as shown in Figure 15.

In this particular search geometry, the target-searcher approaching angle γ is only affected by the target and searcher speeds with its value being calculated using Equation 4.4.

$$\gamma = \arctan \frac{\|\vec{u}\|}{\|\vec{v}\|} \quad (4.4)$$

As the searcher speed increases, with a fixed target speed, γ becomes smaller, as illustrated in Figure 16.

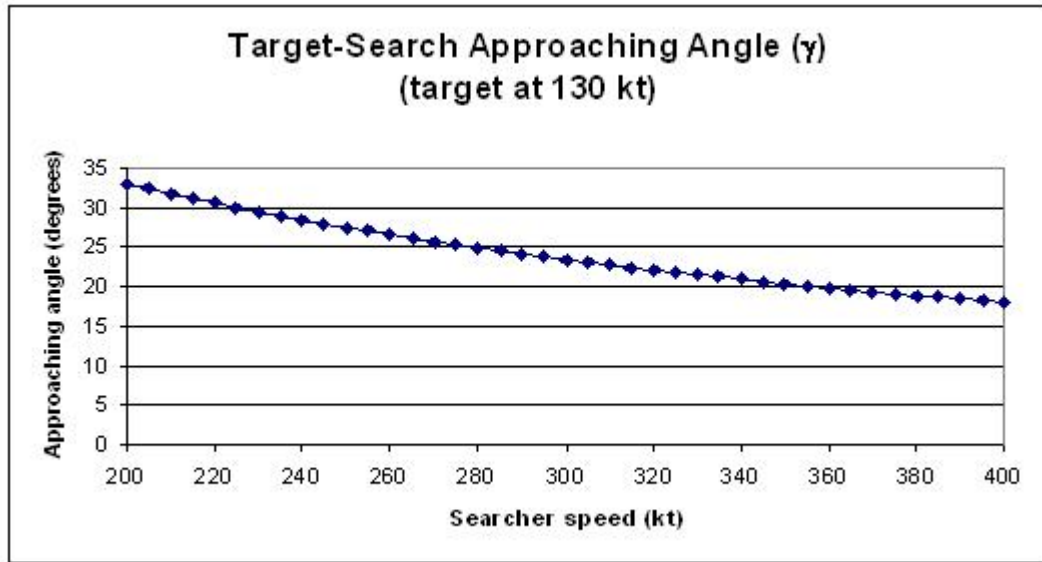


Figure 16. Target-Searcher Approaching Angle Variation

As a result, each target-searcher speed combination must be calculated to verify the γ value prior to any other calculation step. The target-searcher speed ratio of 0.36397 is the minimum value in which γ is greater than the horizontal silence radar angle ϕ . This means that further searcher speed increments, at a fixed target speed, cause a sweep width decrease. This fact is illustrated in Table 1.

The Figure 17 shows the dynamic profile from the target point of view. The shaded area represents the swept area. Since the speeds are constant, the area ratio will be the same for any cycle. Therefore, to facilitate calculating the CDP, the ratio is based on a half cycle. The total searched area corresponds to the rectangle with a base d and a height $L/2$ equal to the distance traveled by the target during a corresponding half cycle performed by the searcher.

u (kt)	v (kt)	ratio	θ (degrees)	w (nm)
130	320	0.40625	22.11	240.0
130	325	0.4	21.80	240.0
130	330	0.393939	21.50	240.0
130	335	0.38806	21.21	240.0
130	340	0.382353	20.92	240.0
130	345	0.376812	20.65	240.0
130	350	0.371429	20.38	240.0
130	355	0.366197	20.11	240.0
130	360	0.361111	19.86	239.7
130	365	0.356164	19.60	239.3
130	370	0.351351	19.36	238.8
130	375	0.346667	19.12	238.4
130	380	0.342105	18.89	238.0
130	385	0.337662	18.66	237.6
130	390	0.333333	18.43	237.2
130	395	0.329114	18.22	236.8

Table 1. Target-Searcher Speed Ratio and Sweep Width Effect

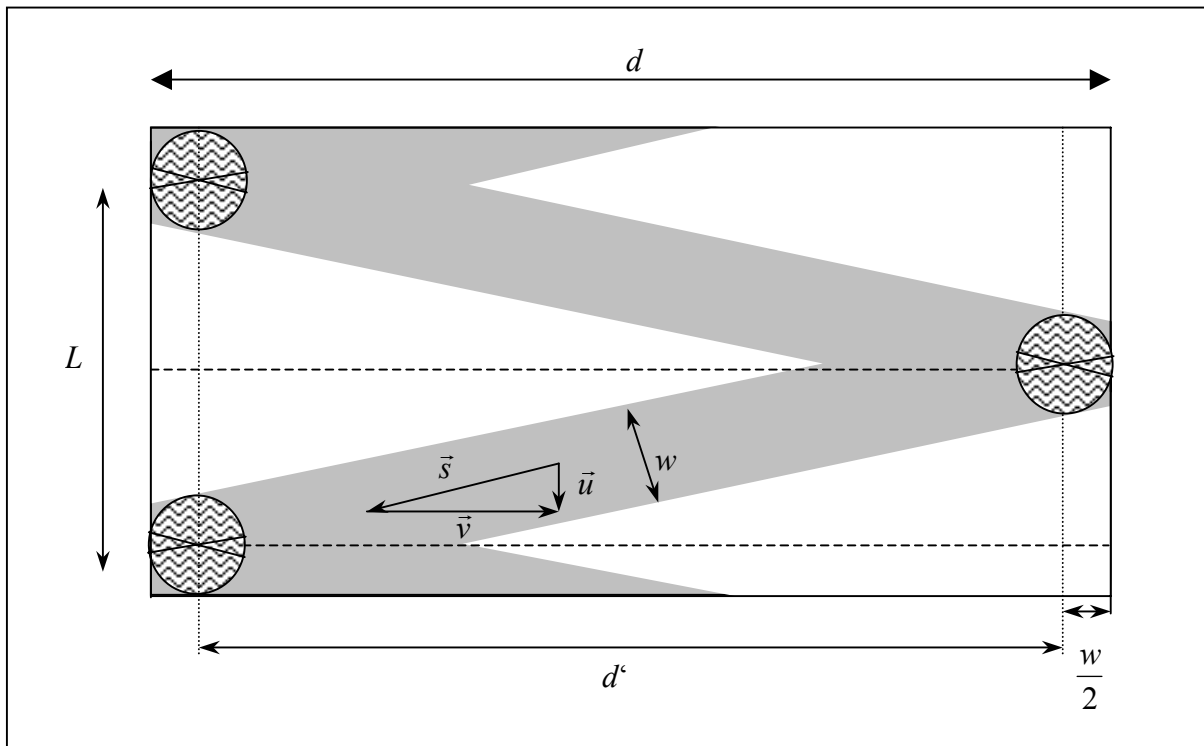


Figure 17. Symmetric Linear Patrol Dynamics

Instead of describing all necessary steps to simplify the ratio of both areas to achieve a closed formula to CPD [10], only the final result, which will be used in further considerations. To differentiate the CDP of each profile, linear and crossover, the acronym $P_{d,L}$ is used to represent the cumulative detection probability of a linear profile search, which respective formula is presented below:

$$P_{d,L} = \begin{cases} 1 - \left[\lambda - \frac{\sqrt{\rho^2 + 1} - 1}{2} \right]^2 \frac{1}{\lambda(\lambda + 1)} & \text{if } \rho \leq 2\sqrt{\lambda(\lambda + 1)} \\ 1 & \text{otherwise} \end{cases} \quad (4.5)$$

where, $\lambda = \frac{(d - w)}{w}$ and $\rho = \frac{\|\vec{v}\|}{\|\vec{u}\|}$

2. Results

A complete spreadsheet was prepared to support the sensitivity profile analysis around the Equation 4.5. Figure 18 shows an extract of such a spreadsheet. All mentioned variables are considered in the computations so that, besides the specific outcomes for this specific case, the interface can assess a complete range of possible profiles used by both, target and searcher.

Searcher FL	28000									
R_max	120	120	120	120	120	120	120	120	120	120
Rmin_hor	51.73124	51.73124	51.73124	51.73124	51.73124	51.73124	51.73124	51.73124	51.73124	51.73124
CPA_null	0	0	0	0	0	0	0	0	0	0
w	240	240	240	240	240	240	240	240	240	240
d	500	500	500	500	500	500	500	500	500	500
d'	260	260	260	260	260	260	260	260	260	260
p	1.38	1.42	1.46	1.50	1.54	1.58	1.62	1.65	1.69	1.73
u	130	130	130	130	130	130	130	130	130	130
v	180	185	190	195	200	205	210	215	220	225
γ	35.84	35.10	34.38	33.69	33.02	32.38	31.76	31.16	30.58	30.02
φ	20	20	20	20	20	20	20	20	20	20
λ	1.08	1.08	1.08	1.08	1.08	1.08	1.08	1.08	1.08	1.08
depth	187.8	182.7	177.9	173.3	169.0	164.9	161.0	157.2	153.6	150.2
P _{d,L}	0.76	0.77	0.78	0.79	0.80	0.81	0.82	0.83	0.84	0.85

Figure 18. Linear Profile Computations

Although the target speed is assumed to be 150 kt, a plot (Figure 19) including a range of speeds around that value was set to give a trend of that variable. The plot shows the CDP at different target and searcher speed combinations. As observed, the slower the target and the faster the searcher, the greater achieved CDP. Therefore, differential speed means more probability of detection. For this particular, an increase of 100 kt in the searcher speed, for a constant target speed, increases the CDP in approximately 15%. On the other hand, an increase in 60 kt in the target speed, for a constant searcher speed, decreases the CDP in approximately 15%. Another significant characteristic of this profile is that it doesn't achieve CDP equals 1 for most combinations illustrated in Figure 19. This results holds whenever the borderline have the extension assumed previously.

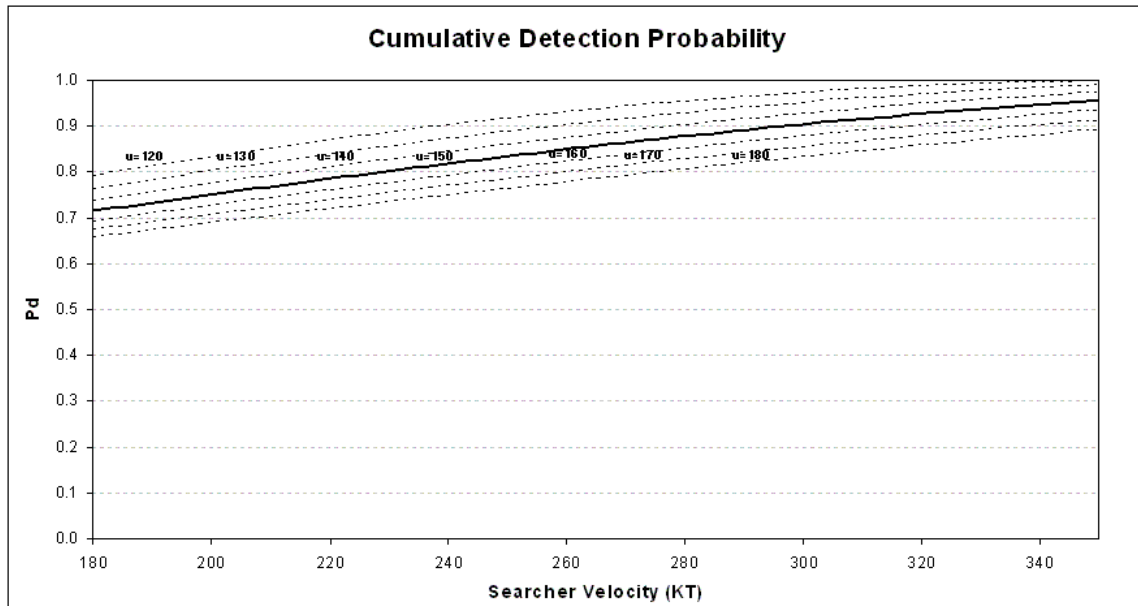


Figure 19. Linear Patrol CDPs – Searcher at 5780 ft

At this point is opportune to say that those resulting probabilities are conditioned in known speeds. If a reasonable doubt exists about that parameter, a conditional probability of detection has to include the entire range of possible target speed values. That computation is easily accomplished since the target speed probability density function is available. This fact was mentioned to avoid the attempt of using the mean of

those plotted probabilities at different speeds to solve the problem cited in the previous period. The results will not correspond to the truth if the later procedure is adopted.

Although the target-speed ratio has decreasing influence in the sweep width when this ratio is smaller than 0.36397, the CDP still has increasing values. Therefore, even causing smaller sweep width, differential speed still increases the overall CDP. Table 2 illustrates this situation.

u (kt)	v (kt)	ratio	θ (degrees)	w (nm)	CDP
130	320	0.40625	22.11	240.0	0.971
130	325	0.4	21.80	240.0	0.975
130	330	0.393939	21.50	240.0	0.979
130	335	0.38806	21.21	240.0	0.982
130	340	0.382353	20.92	240.0	0.985
130	345	0.376812	20.65	240.0	0.988
130	350	0.371429	20.38	240.0	0.990
130	355	0.366197	20.11	240.0	0.993
130	360	0.361111	19.86	239.7	0.994
130	365	0.356164	19.60	239.3	0.996
130	370	0.351351	19.36	238.8	0.997
130	375	0.346667	19.12	238.4	0.998
130	380	0.342105	18.89	238.0	0.999
130	385	0.337662	18.66	237.6	1.000
130	390	0.333333	18.43	237.2	1.000
130	395	0.329114	18.22	236.8	1.000

Table 2. Target-Speed Ratio Effects on CDP

Another important result is that the searcher altitude barely improves the CDP. A minor effect can be noted, for instance, at target speed of 150 kt and at searcher speed of 405 kt. Figure 20 illustrates this fact. In this situation, the target-searcher speed ratio is slightly smaller than the limit mentioned previously. This results in the CDP of this profile being viewed as practically independent of the searcher altitude.

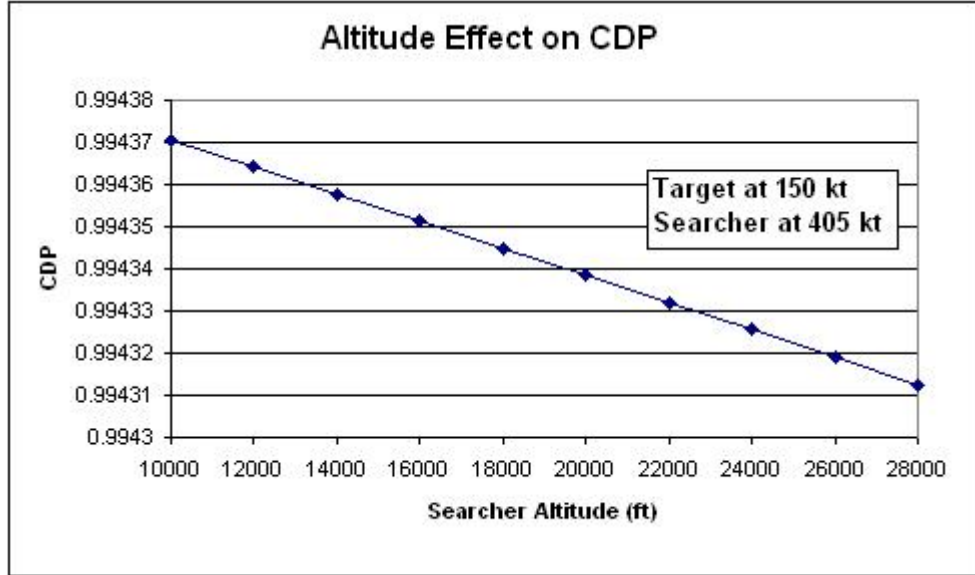


Figure 20. Altitude Effect on Linear Profile CDP

In the next topic, the second barrier patrol type is detailed.

D. SYMMETRIC CROSSOVER PATROL

1. Search Geometry

In this pattern, instead of back and forth profiles, the searcher performs a cross orbit, as illustrated in Figure 21.

Unlike the preceding geometry, here the searcher path is dependent of the target speed. Between the leg AB and the perpendicular line to the target path exists an angle γ . This angle is derived from a hypothetical meeting of searcher and target at point B, as illustrated in Figure 22 and takes different values according the following relationship:

$$\gamma = \arcsin \frac{\|\vec{u}\|}{\|\vec{v}\|} \quad (4.6)$$

Therefore, given a target speed, the searcher must flies in a direction to achieve this angle, according the selected patrolling speed, so that the Equation 4.6 holds the equality. Additionally, since γ is also the target-searcher approaching angle, the searcher can vary its speed to move the target approaching path out of the radar silence zone. This

procedure guarantees a better sweep with as illustrated in Table 3, where decreasing the searcher speed from 385 kt to 380 kt improves w .

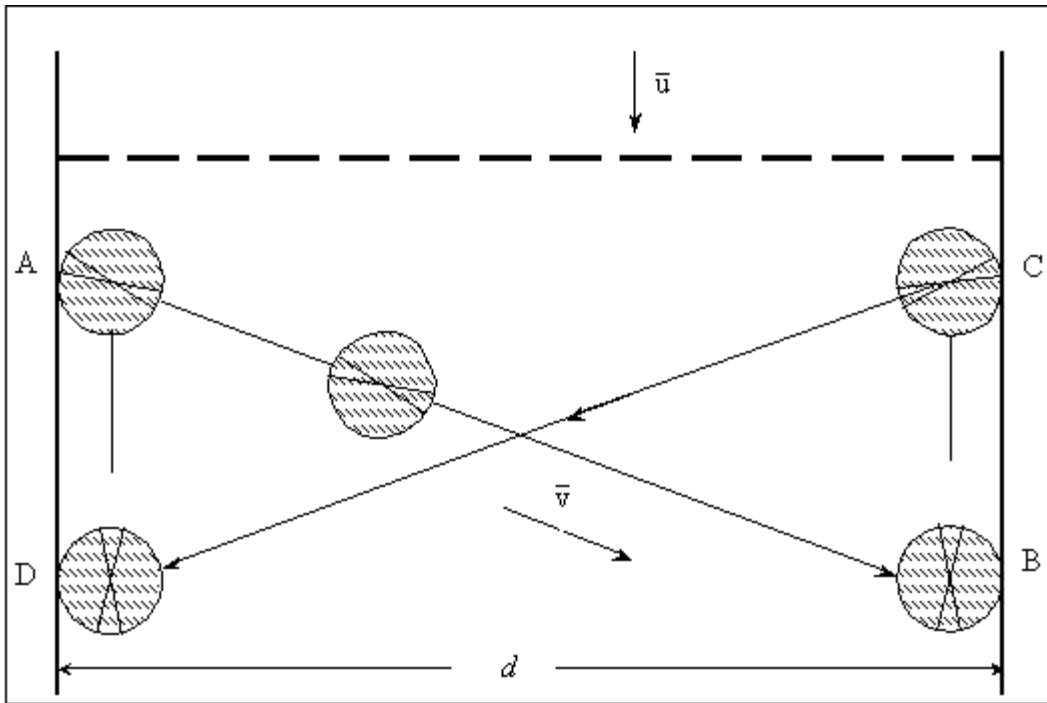


Figure 21. Symmetric Crossover Barrier Patrol Geometry

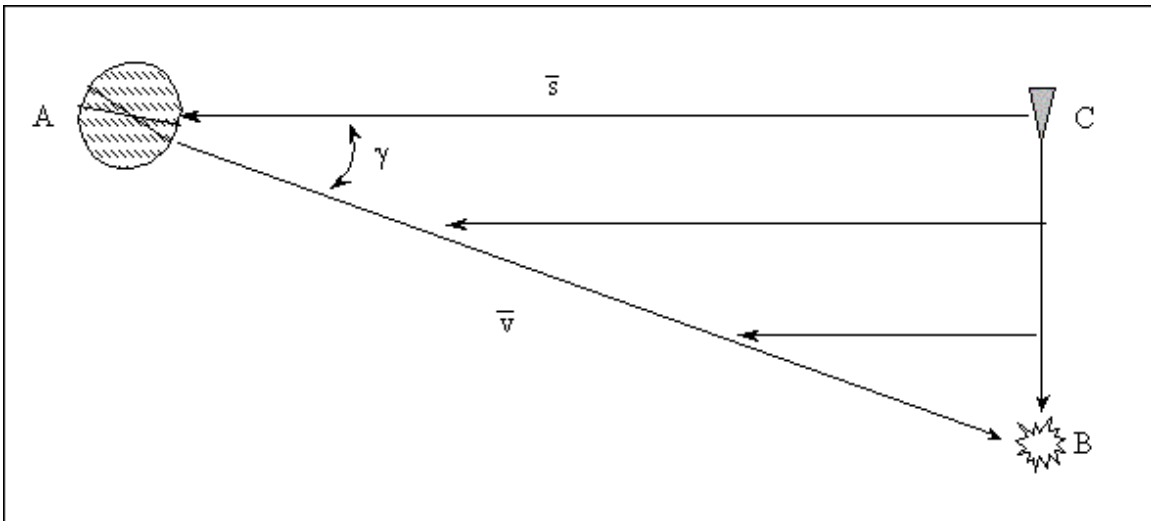


Figure 22. Crossover Barrier Patrol – Cross-Angle

u	v	u/v	γ (degrees)	w
100	300	0.33	19.5	240.0
100	370	0.27	15.7	240.0
100	375	0.27	15.5	240.0
100	380	0.26	15.3	240.0
100	385	0.26	15.1	239.6
100	390	0.26	14.9	239.3
100	395	0.25	14.7	238.9
100	400	0.25	14.5	238.5

Table 3. Searcher Speed and Sweep Width Variation

After reaching point B, the searcher goes to point C. Critical part of patrol is between these two points because the target-searcher's approaching angle will be null. This decreases the sweep width to its lowest value possible to a given searcher altitude. This fact is observable at Figure 23. The black area corresponds to the coverage lost due to the decrease in the sweep width. The dashed area is that area effectively swept by the sensor and the gray area is that covered in the crossing legs.

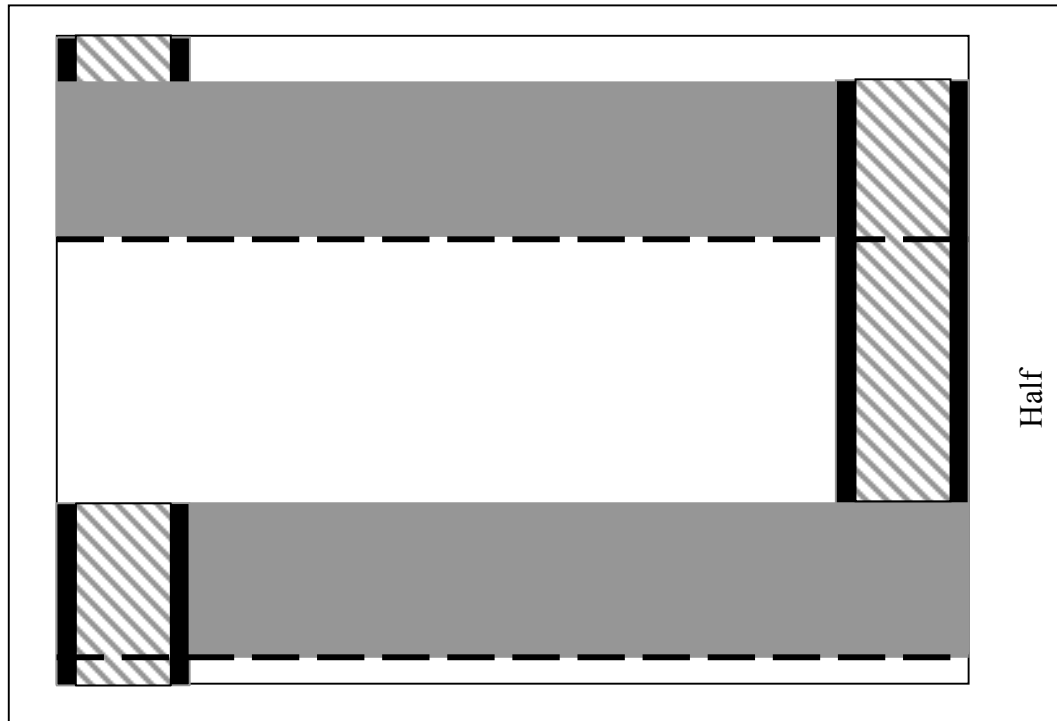


Figure 23. Crossover Barrier Patrol Dynamics

This fact shows that the crossover profile's CDP ($P_{d,C}$) cannot be calculated using Equation 4.7 [10] for this kind of sensor. The parameters nomenclature is the same used in the linear case.

$$P_{d,C} = \min \left\{ 1, \left(1 + \frac{\rho \sqrt{\rho^2 - 1}}{\rho + 1} \right) \frac{1}{\lambda + 1} \right\} \quad (4.7)$$

The previous formula holds the same principle about the probability of detection; that is, the result comes from the ratio between the total searched area and the swept area.

Instead of a normal sweep width, a reduced sweep has to be used in the calculations to find the area traveled by the searcher in the opposite direction of the target. Consequently that area will have a height equal to the distance traveled by the target during the half cycle and a width equivalent to the reduced sensor sweep width, as described below:

$$\text{Sweep Area} = (d - w) + \left[\frac{d - w}{\sqrt{\rho^2 - 1}} + \frac{d - w}{\rho \sqrt{\rho^2 - 1}} \right] w_R \quad (4.8)$$

where, w_R is the reduced sweep width.

The only difference in the area calculation used in the proposed modified version from the Equation 4.7 is the very last term, w_R . By dividing Equation 4.8 by the total searched area, the following formula is obtained:

$$P_{d,C \text{ mod}} = \min \left\{ 1, \left(\frac{w_R}{w} + \frac{\rho \sqrt{\rho^2 - 1}}{\rho + 1} \right) \frac{1}{\lambda + 1} \right\} \quad (4.9)$$

The resulting formula is quite close to the original with a difference in the appearance of the ratio $\frac{w_R}{w}$ in substitution for the number 1. As a consequence, every

time the sweep width is decreased in the up (down) leg, a lost occurs in the resulting CDP. Otherwise, the ratio becomes 1 and the original equation (4.7) is reestablished.

2. Results

The same spreadsheet used in the linear patrol CDP computations also includes the outcomes for the crossover patrol CDP, shown below.

Searcher FL	28000								
R_max	120	120	120	120	120	120	120	120	120
Rmin_hor	51.73	51.73	51.73	51.73	51.73	51.73	51.73	51.73	51.73
CPA_null	0	0	0	0	0	0	0	0	0
CPA_null'	17.69	17.69	17.69	17.69	17.69	17.69	17.69	17.69	17.69
w	240	240	240	240	240	240	240	240	240
w'	204.6137	204.6137	204.6137	204.613746	204.6137	204.6137	204.6137	204.6137	204.6137
d	500	500	500	500	500	500	500	500	500
d'	260	260	260	260	260	260	260	260	260
p	1.06	1.09	1.12	1.15	1.18	1.21	1.24	1.26	1.29
u	170	170	170	170	170	170	170	170	170
v	180	185	190	195	200	205	210	215	220
γ	70.81	66.77	63.47	60.67	58.21	56.02	54.05	52.25	50.60
γ'	0	0	0	0	0	0	0	0	0
φ	20	20	20	20	20	20	20	20	20
λ	1.08	1.08	1.08	1.08	1.08	1.08	1.08	1.08	1.08
deep	747.1	605.7	520.9	462.7	419.5	385.8	358.5	335.8	316.5
Pd	0.50	0.52	0.54	0.55	0.57	0.59	0.60	0.62	0.63
Opt_d	247.57	258.30	267.84	276.66	285.01	293.03	300.80	308.38	315.82

Figure 24. Crossover Profile Computations

As expected, the results indicate an effect of altitude in the CDP. The higher the searcher's altitude, the lower is the CDP. This fact holds whenever the searcher's altitudes are greater than the optimal coverage altitude (5775 ft). Below this altitude, the effect is contrary; that is, lower searcher's altitudes result in smaller CDPs. Figure 25 illustrates this scenario

Although large speed's difference between searcher and target cause decrease in the sweep width in circumstances as illustrated in Table 3, the overall CDP is always greater for faster searcher's speeds. This fact is observed in Figure 26.

The last and important feature of this design is that CDPs equals 1 are more likely to occur in crossover geometry than in the linear geometry. The next topic of this chapter is dedicated to compare both designs characteristics.

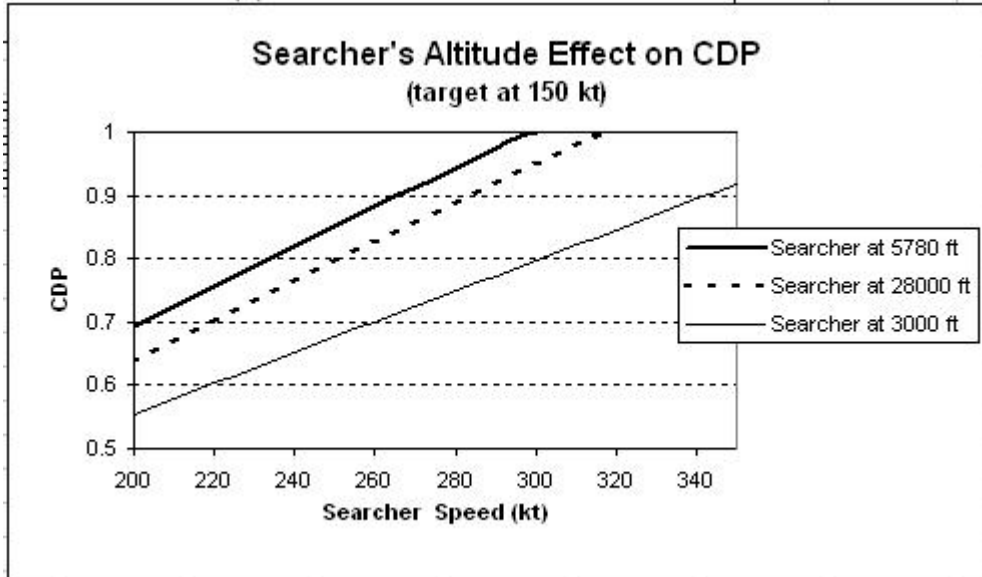


Figure 25. Effect of Altitude on Crossover CDPs

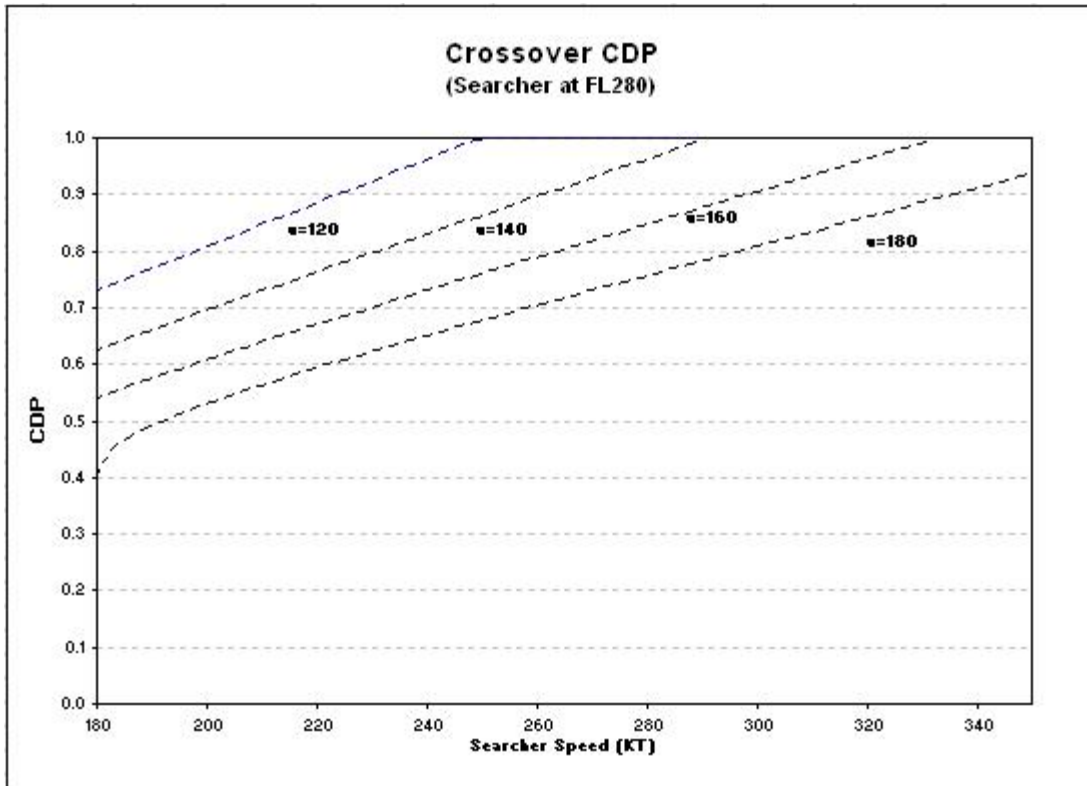


Figure 26. Crossover Barrier Patrol CDPs- Searcher at 28000 ft

E. PATROL PATTERN COMPARISONS

Some important differences between the two patrol patterns deserve close attention.

1. Searcher Speed Effects

In the linear patrol design, the CDP for a given target speed has a low variation as the searcher increases its speed. For the range in question, the CDP only increased at most by 20%. However in the crossover design, the searcher speed parameter had a strong effect in the achieved CDP. As observed in Figure 26, the CDP jumped from .4 to .8 as the searcher increased the speed from 180 to 300 kt. This is, a 100% CDP improvement.

2. Relative Speed Effects

Another evident distinction between both patterns is also related to speed. As shown in Figure 27, given a target speed, the linear profile achieves greater CDP from lower searcher speeds up until a point where the crossover design attains better CDP results. This fact was amplified as the targets speeds became larger. Therefore, depending on the speeds of both, target and searcher, a better option exists in terms of patrol profile.

3. CDP Effects

At a target speed of 150 kt, the crossover patrol was the only design that reached a CDP equaling 1. As presented before, the linear patrol pattern achieves better CDP for lower searcher speeds, but is unable to guarantee a target detection probability equal to 1 for the target's assumed speed.

4. Searcher-Altitude Effects

The searcher altitude negatively affected the crossover patrol geometry at flight levels above the optimal coverage altitude (5775 ft); that is, the higher the searcher

altitude, lower the CDP. This fact is illustrated in Figure 25. On the other hand, different searcher's altitudes did not affect the linear patrol geometry's CDP.

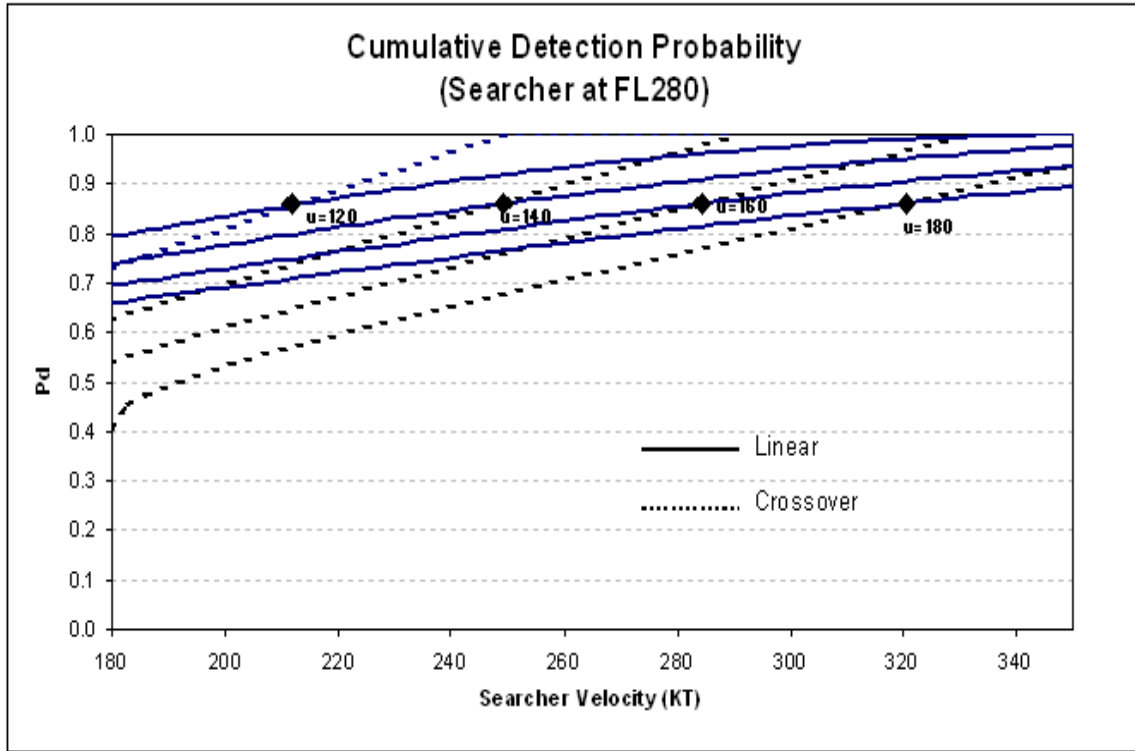


Figure 27. Crossover versus linear barrier patrol.

5. Patrol Area

The portion of space necessary to apply both geometries is also an important aspect to be considered. The linear patrol always requires the same area to be employed. Conversely, the crossover pattern varies with area limits for each target-searcher combination. As observed in the geometry description, the area length was the same for both profiles, but crossover profile was wider than linear design for target speeds greater than 0 kt.

6. Optimum Search Length

Other useful comparisons refer to the maximum search length in which the respective patrol design achieves CDP equals 1, that is, the optimum search length. The

graph in the Figure 28 illustrates that point. Only three target speeds were selected: 130, 150 and 170 kt. The plotted curves showed that at lower searcher speeds, the linear patrol geometry covered larger lengths than the crossover patrol design. The other apparent outcome was that lower target speeds resulted in bigger search lengths.

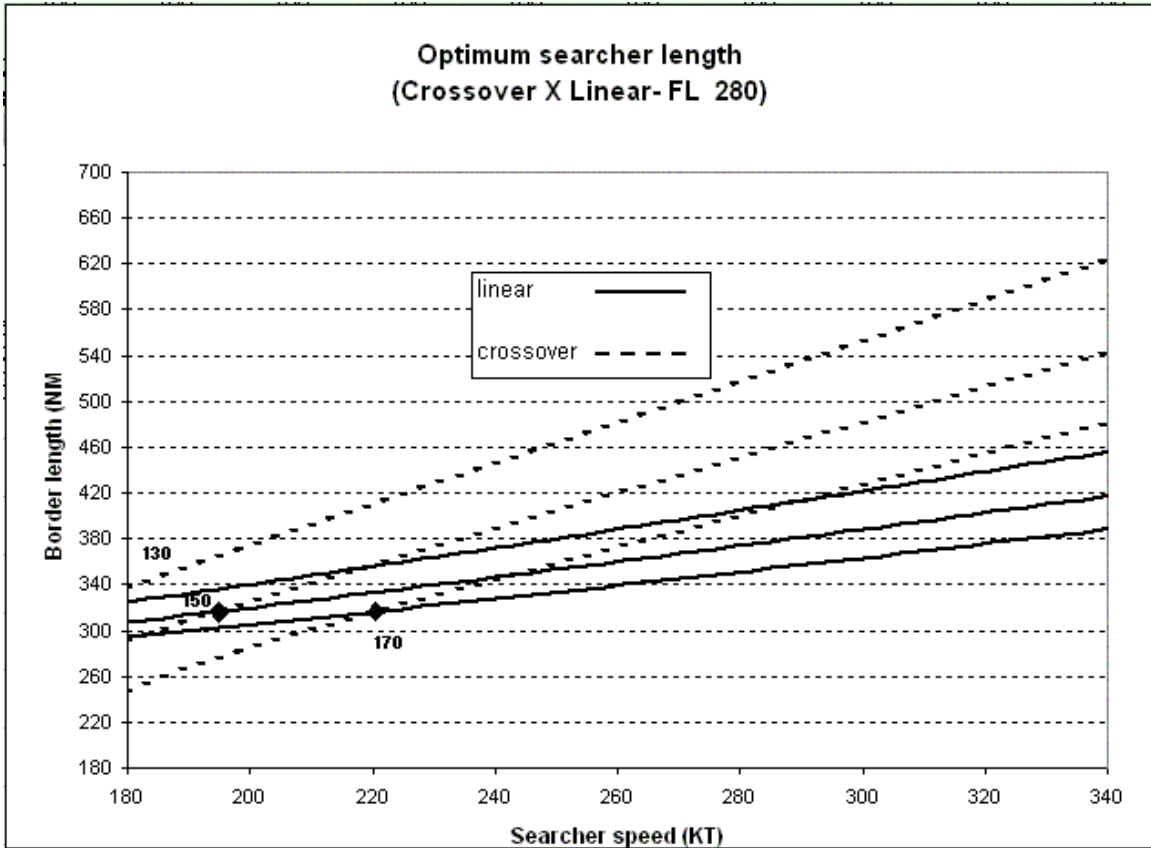


Figure 28. Optimum Search Length Comparison

7. Prior Target Knowledge

The linear design does not depend on previous knowledge of target speed, because the searcher always performs the same path (back and fourth). Conversely, the crossover pattern is set based on previous target speed information. A good estimate can provide a good geometry and more reliable results, but inaccurate target knowledge can cause under or over estimations of CDP.

V. CAMPAIGN DECISION AID

The sensitive analysis achieved in the previous chapter and the proposed scenario assumptions provide most of the necessary information to formulate a method that accomplishes the campaign planning. The missing elements still necessary to complete the planning are those related to the platforms' tactical scenario integration, that is,

CAMPAIGN DECISION AID				
	X Coord	Y Coord		
Air Base 1 Coordinates	10	290		
Air Base 2 Coordinates	430	340		
Available Number Of Searchers	5 UN			
Number of Searchers Engaged	2 UN			
Searcher Ingress Speed	300 KT			
Searcher Egress Speed	310 KT			
Interceptor Speed	340 kt			
Preset Interception Line	290 nm			
Search Length	535 nm			
Campaign Duration	72 h			
Ingress Time to Station		40/60		
Egress Time to Station		39/60		
Expected Ground Time		2		
Additional Ground Time		2		
Max OST Available		7		
Required On Station Time		5 20/60		
Optional On Station Time Between Max and Required OST			5 20/60	
Target Speed		152 kt		
Expected Inter-targets Time		6 h		
PROFILE SUMMARY				
Ideal Profile	Crossover	Expected Crossing Targets	12	
Optimum FL	26000 ft			
Optimum Searcher Speed	320 kt			
CDP	0.95			
Station-Base Distance	202.5 nm			
Search Depth	399.2 nm			
Actual On Station Time	5 20/60 h			
Actual Searchers Engaged	2			
Actual Search Length	535.0 nm			
		Base 1	Base 2	Both
Expected Tgts Lost	GLI	1.98	1.68	1.34
	CAP	0.59	0.59	0.59
Expected Tgts	GLI	10.02	10.32	10.66
Detected-Chased	CAP	11.41	11.41	11.41
Percentage Interceptable Tgts		0.45	0.52	0.62

Figure 29. Campaign Decision Aid User Interface

basically, geographic placement effects, for both searchers and interceptors. Obviously, the ideal plan would be one where many searchers occupy small distinct regions in order to guarantee cumulative detection probability (CDP) equal 1 in the whole area of interest and where interceptors always perform combat air patrol (CAP) minimizing the reaction time. Nonetheless, this solution is not feasible since resources are limited. A balanced plan, therefore, is necessary to better utilize the available resources while achieving an acceptable result. The suggested approach to reach such a purpose is the Campaign Decision Aid (CDA), whose user's spreadsheet interface is shown in Figure 29. The

CDA is formulated using a sequence of prioritized steps: searcher's minimum availability, searcher's profile selection and campaign's measures of effectiveness. These steps are described in the following sub topics.

A SEARCHER'S MINIMUM AVAILABILITY

The number of searchers required in the campaign is the starting point of the CDA. In the assumed scenario, an uninterrupted and intense campaign is established to detain the most possible number of illegal aircraft in a limited campaign period. Achieving that task requires at least one searcher constantly over the area of interest. This implies the availability of at least two searchers to be engaged sequentially and uninterruptedly in the area of interest; that is, a searcher has to arrive in the named area of interest at the moment the other searcher is leaving the same area. The computation necessary to assure the profile mentioned above is based on the following equation:

$$I + E + B + A = S \times (N - 1) \quad (5.1)$$

or, solving by S :

$$S = \frac{I + E + B + A}{N - 1}$$

where:

I = searcher's flight time from its base to the named area of interest

E = searcher's flight time from the named area of interest to its base

B = time between last landing and the next searcher take-off

A = extra time between last landing and the next searcher take-off

N = number of needed searchers engaged in the mission

S = required on station time

On the left hand side of the equation 5.1, I represents the searcher's flight time from its base to the named area of interest while E represents the egress time to its base. These two parameters are solved based in the searcher's speed used in the corresponding

situation and on the distance between the patrolling area and the searcher deployed Air Base.

	X Coord	Y Coord
Air Base 1 Coordinates	10	290
Air Base 2 Coordinates	430	340

Figure 30. Air Bases Coordinates Entry

The CDA provides this distance after the user sets the Air Base 1 coordinates in the specified field (Figure 30). The coordinates' reference originates in the search polygon corner closest to the borderline and to the patrolling starting point. The orientation is positive in right and in the Brazilian interior directions as illustrated in Figure 31.

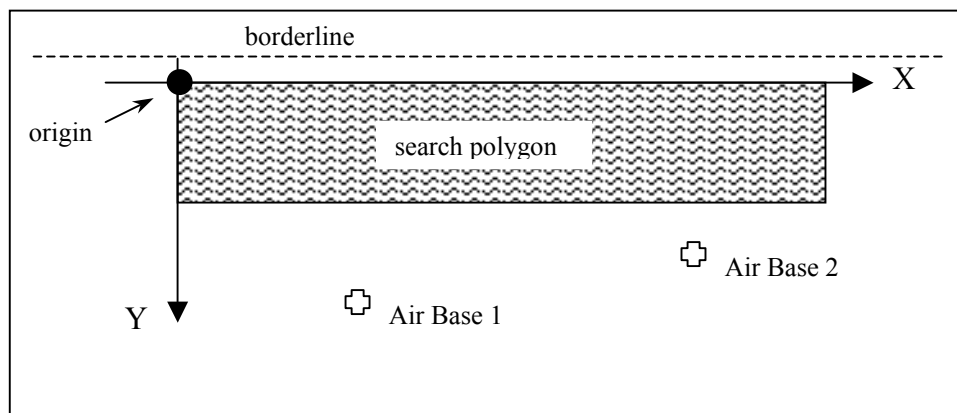


Figure 31. Coordinates' Referential Description

The term B is the time between last landing and the next searcher take-off (aircraft on base). This calculation is an average time spent in pre-flight maintenance activities like refueling and routine inspections between two consecutive flights. In this thesis, the schedule maintenance activities to occur in a predetermined number of flight hours are assumed to be executed before the campaign begins. This assumption is quite reasonable, since this anticipating procedure is adopted in current deployments. This procedure is done to decrease the logistic support required for the mission and to avoid availability restrictions. Another assumption related to B is its value, which is set in 2 hours.

In the left hand side of equation 5.1, the remaining term A represents extra time to be set by the campaign's planner according to need, for instance, increasing the crew resting period. There is no underlying probability distribution to A and the only requirement in terms of planning is observing the selected time during the whole campaign.

In the right hand side of equation 5.1, N corresponds to the number of needed searchers engaged in the mission. As a result no interruption occurs in patrolling; therefore, the minimum value for this parameter is 2.

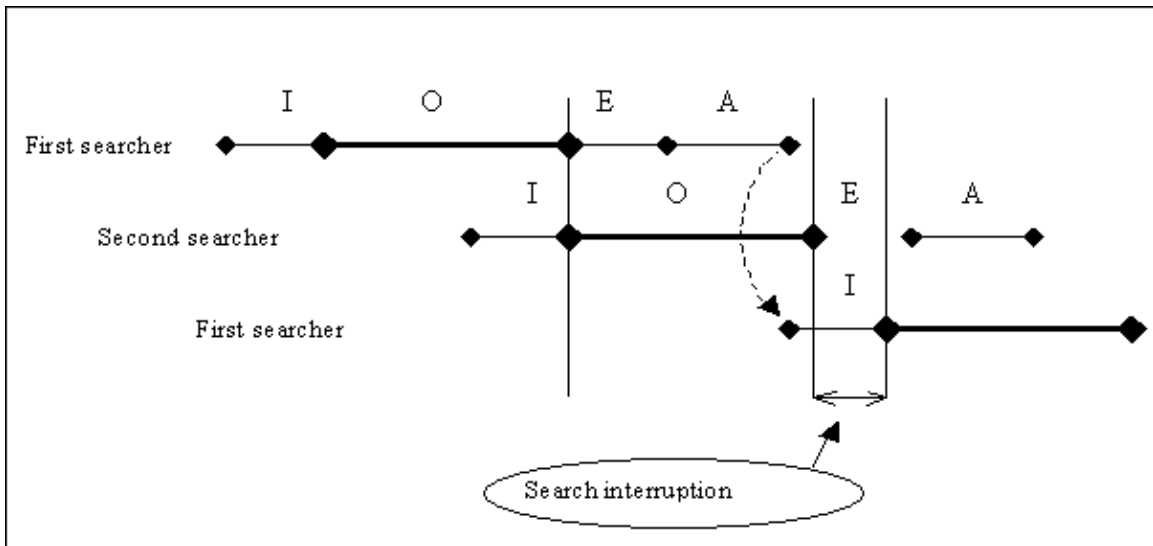


Figure 32. Infeasible On Station Time

The last term of equation 5.1, S , represents the required on station time. If S is smaller than the maximum available on station time O , the profile is not feasible, considering the specified N . Therefore, to solve this infeasibility, the number of engaged searchers has to increase or one of the parameters in the left hand side of 5.1 has to decrease. Figure 32 illustrates the situation where the available on station time is smaller than the required on station time, causing an interruption in the search.

The Figure 33 illustrates a feasible search where a third searcher was added to eliminate the search interruption.

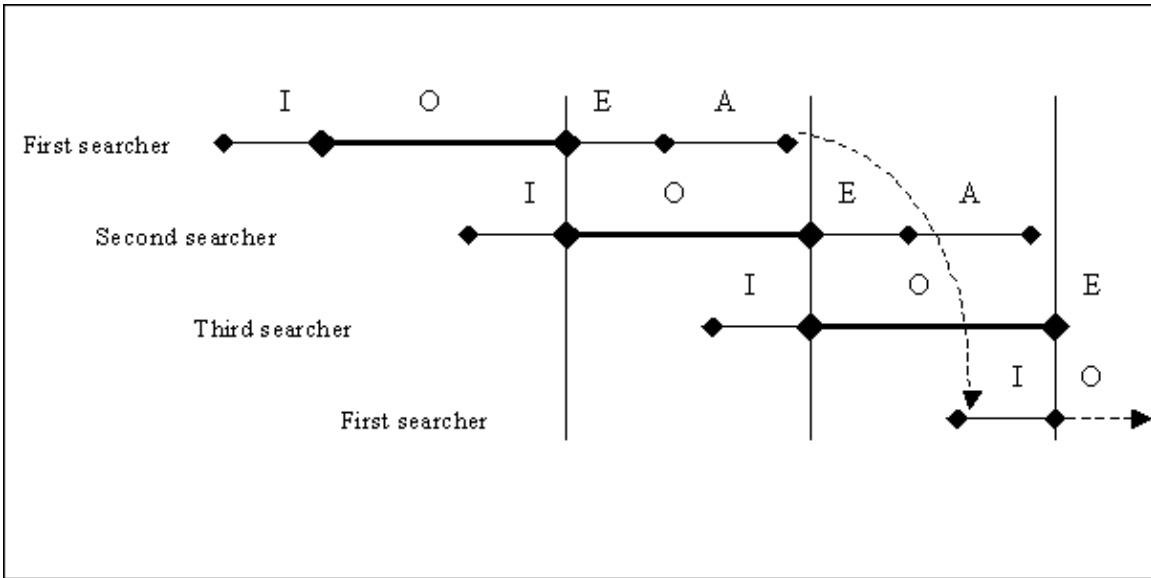


Figure 33. Feasible On Station Time After Adding Third Searcher

The available time on station *O* results by subtracting *E* and *I* from the maximum available time in a specific flight profile, that is, in the searcher predetermined speed and altitude. Table 4 shows the maximum available times to the respective flight profiles, which is function of aircraft’s fuel capacities. As observed, this is a simplified sample that will be the basis for the computations involving on station time calculations in this thesis.

Figure 34 shows, in the white cells, the feasible profiles and their respective available on station times. Each cell supposes that *S* is 5:20 hours and the summation of *I* and *E* is 1:20 hours. The CDA user interface presents the mentioned parameters and the resulting required on station time in the right-top position as illustrated in Figure 35.

Altitude	Searcher Speed								
	180	200	220	240	260	280	300	320	340
6000	5.58	5.33	5.08	4.92	4.83	4.67	4.17	3.92	3.50
8000	5.92	5.75	5.33	5.17	5.00	4.83	4.58	4.17	3.83
10000	6.25	6.00	5.83	5.58	5.33	5.08	4.92	4.58	4.08
12000	6.58	6.33	6.08	5.83	5.67	5.33	5.08	4.83	4.50
14000	6.83	6.58	6.33	6.08	5.92	5.67	5.25	5.00	4.75
16000	7.08	6.92	6.75	6.42	6.17	5.83	5.42	5.25	4.92
18000	7.25	7.08	6.83	6.75	6.50	6.17	5.92	5.67	5.33
20000	7.42	7.25	7.00	6.83	6.75	6.42	6.08	5.83	5.58
22000	7.67	7.58	7.33	7.17	6.92	6.67	6.25	6.00	5.75
24000	7.92	7.83	7.67	7.42	7.17	6.92	6.50	6.25	6.00
26000	8.17	8.08	7.92	7.75	7.50	7.17	7.00	6.75	6.33
28000	8.33	8.25	8.08	7.92	7.75	7.42	7.08	6.83	6.58

Table 4. Searcher’s Maximum Available Flight Times (hours)

Altitude	Searcher Speed								
	180	200	220	240.00	260	280	300	320	340
6000	4.26	4.01	3.76	3.59	3.51	3.34	2.84	2.59	2.17
8000	4.59	4.42	4.01	3.84	3.67	3.51	3.26	2.84	2.51
10000	4.92	4.67	4.51	4.26	4.01	3.76	3.59	3.26	2.76
12000	5.26	5.01	4.76	4.51	4.34	4.01	3.76	3.51	3.17
14000	5.51	5.26	5.01	4.76	4.59	4.34	3.92	3.67	3.42
16000	5.76	5.59	5.42	5.09	4.84	4.51	4.09	3.92	3.59
18000	5.92	5.76	5.51	5.42	5.17	4.84	4.59	4.34	4.01
20000	6.09	5.92	5.67	5.51	5.42	5.09	4.76	4.51	4.26
22000	6.34	6.26	6.01	5.84	5.59	5.34	4.92	4.67	4.42
24000	6.59	6.51	6.34	6.09	5.84	5.59	5.17	4.92	4.67
26000	6.84	6.76	6.59	6.42	6.17	5.84	5.67	5.42	5.01
28000	7.01	6.92	6.76	6.59	6.42	6.09	5.76	5.51	5.26

Figure 34. Feasible On Station Time Profiles

Ingress Time to Station	40/60
Egress Time to Station	39/60
Expected Ground Time	2
Additional Ground Time	2
Max OST Available	7
Required On Station Time	5 20/60

Figure 35. Required On Station Time

B. SEARCHER'S PROFILE SELECTION

From the feasible profiles presented in Figure 34, another grid is generated, as illustrated in Figure 36.

CROSSOVER					LINEAR				
CDP	opt_level	opt_speed	depth	length	CDP	opt_level	opt_speed	depth	length
0.00					0.00				
0.00					0.00				
0.00					0.00				
0.00					0.00				
0.57					0.67				
0.69					0.74				
0.74					0.77				
0.79					0.80				
0.85					0.83				
0.84					0.83				
0.95	26000	320	399.24	535.00	0.88				
0.94					0.88	28000	320	240	535

Figure 36. Searcher Profile Selection

In this illustration, the CDPs corresponding to the feasible profiles are computed and the biggest CDP of each patrolling geometry is selected. The next step picks the greatest

CDPs between the two geometries and computes all parameters of interest like optimum flight level, optimum speed, search depth and length. These parameters are then presented in the left-bottom portion of CDA user interface (Figure 37).

Ideal Profile	Crossover
Optimum FL	26000 ft
Optimum Searcher Speed	320 kt
CDP	0.95
Station-Base Distance	202.5 nm
Search Depth	399.2 nm
Actual On Station Time	5 20/60 h
Actual Searchers Engaged	2
Actual Search Length	535.0 nm

Figure 37. Search Profile Summary

C. CAMPAIGN’S MEASURES OF EFFECTIVENESS

There are several methods to evaluate the effectiveness of the campaign. The CDP and on station time are good measures of effectiveness (MOEs) for searchers, but they do not reflect the campaign’s integrated effort. Since the campaign’s final objective is to detain the illicit traffic, the measures of effectiveness raised in this thesis are related to the capability of intercepting the detected targets. In order to illustrate the method used to generate these measures of effectiveness of the campaign, some considerations about interception reaction time are necessary.

Intercepting the target can be achieved from two different initial situations. In the first, the interceptor is placed in flight around the search aircraft, that is, in a combat air patrol (CAP). Since the detections occur inside the volume around the search aircraft and the interceptor occupies a position inside the same space, the time to intercept a detected target is assumed negligible. As a result, the search aircraft is not needed to chase the detected target to support the interception while the patrolling is not interrupted.

In the second case, the interceptor stands by for the launch in a pre-determined Air Base, which is called a ground launch interception (GLI). This situation requires more attention since the interception depends on a combination of factors. As soon as the

detection occurs, the interceptor is launched towards the target. This scenario is illustrated in Figure 38. If the interceptor flies with a speed $\|\vec{i}\|$, and the target flies with a speed $\|\vec{u}\|$, the interception is will to take place at a point in the interior of Brazilian territory.

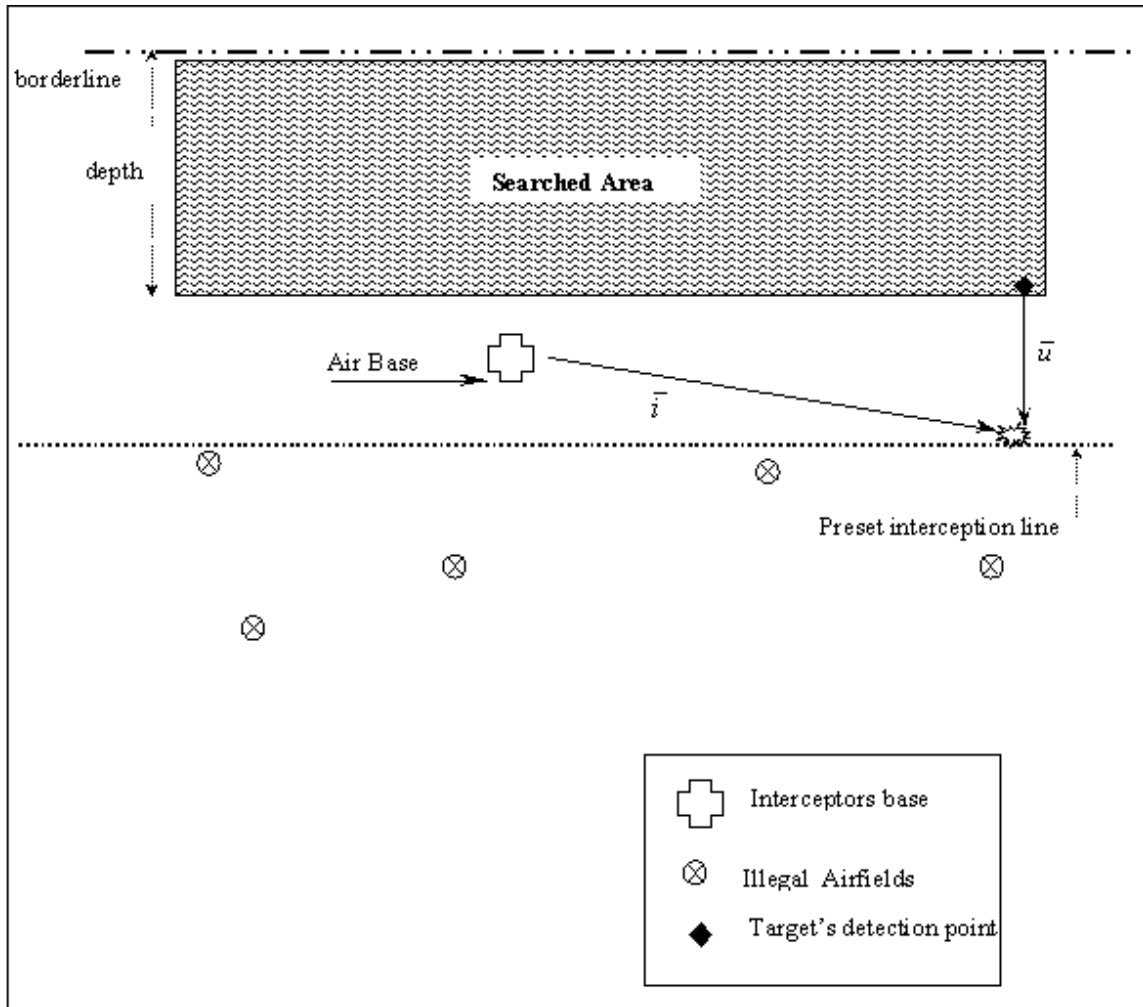


Figure 38. Reaction Time Factors

The preset interception line illustrated in Figure 38 represents a limit established as a function of existing illegal airfields in the region of interest. Intelligence activity is necessary before the campaign begins to identify the illegal airfields' location. If a target crosses the preset interception line, it will be able to land at the destination before the interception occurs. Therefore, some detected targets will not be intercepted because the

GLI reaction time will be greater than the target's flight time from its detection to the preset interception line.

Two factors contribute to the GLI reaction time. The interceptor Air Base's location is one of these factors since it determines the distance to reach a detected target. Another factor is the interceptor speed. Figure 39 illustrates the interception problem in which y_0 is the distance from the target's point of detection until the perpendicular point to the interceptor's Air Base. The term x_0 is the perpendicular distance from the interceptor's Air Base to the target's flight project line. Based on this set up, the following formulation holds:

$$\left(\|\vec{i}\| \cdot t\right)^2 = x_0^2 + \left(\|\vec{u}\| \cdot t - y_0\right)^2 \quad (5.2)$$

where:

i = interceptor velocity

u = target velocity

t = interception time

x_0 = as defined above

y_0 = as defined above

Solving 5.2 by t , the resulting Equation 5.3 gives the time to intercept a detected target at any point within the searched area, and launches the interceptor from a predetermined Air Base. As stated in this formulation, the solution is the minimum positive value encountered after solving this quadratic equation.

$$t = \min \left(-2 \cdot y_0 \cdot \|\vec{u}\| \pm \sqrt{(2 \cdot y_0 \cdot \|\vec{u}\|)^2 - 4 \left(\|\vec{i}\|^2 - \|\vec{u}\|^2 \right) (x_0^2 + y_0^2)} \right) \quad \{\text{for } t \geq 0\} \quad (5.3)$$

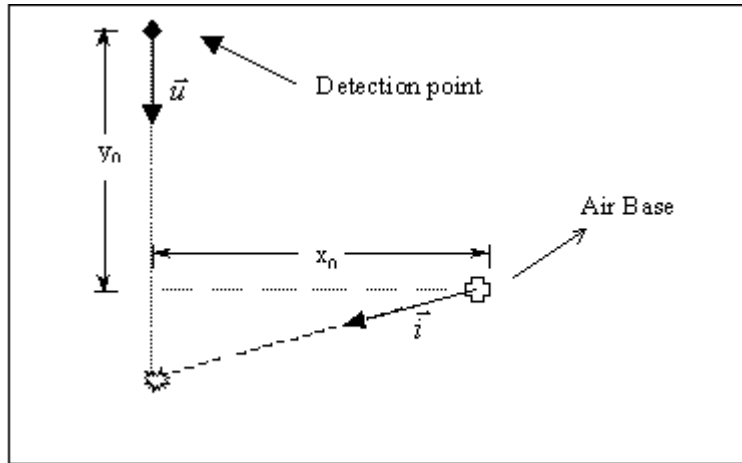


Figure 39. Interception Set up

The expected time of target interception in the area $E[T_i]$ is obtained by integrating the interception times t over all points of detection in the searched area and dividing the result by that same area, as illustrated below in Equation 5.4:

$$E[T_i] = \frac{1}{d \cdot L} \int_0^d \int_0^L t dt \quad (5.4)$$

where:

d = search length

L = search depth

In order to solve such an equation using a spreadsheet, the area was divided in to small rectangles representing the “points” of detection. That is, the continuous Equation 5.4 was transformed into a discrete problem. Figure 40 shows the time to intercept targets detected inside 10x10 nm squares. The time to intercept the target in each square appears inside respective cell.

an exponential distribution with mean $\frac{1}{\beta}$ hours, where β is assumed to be a rate of 6 arriving targets per hour, according to a Poisson process.

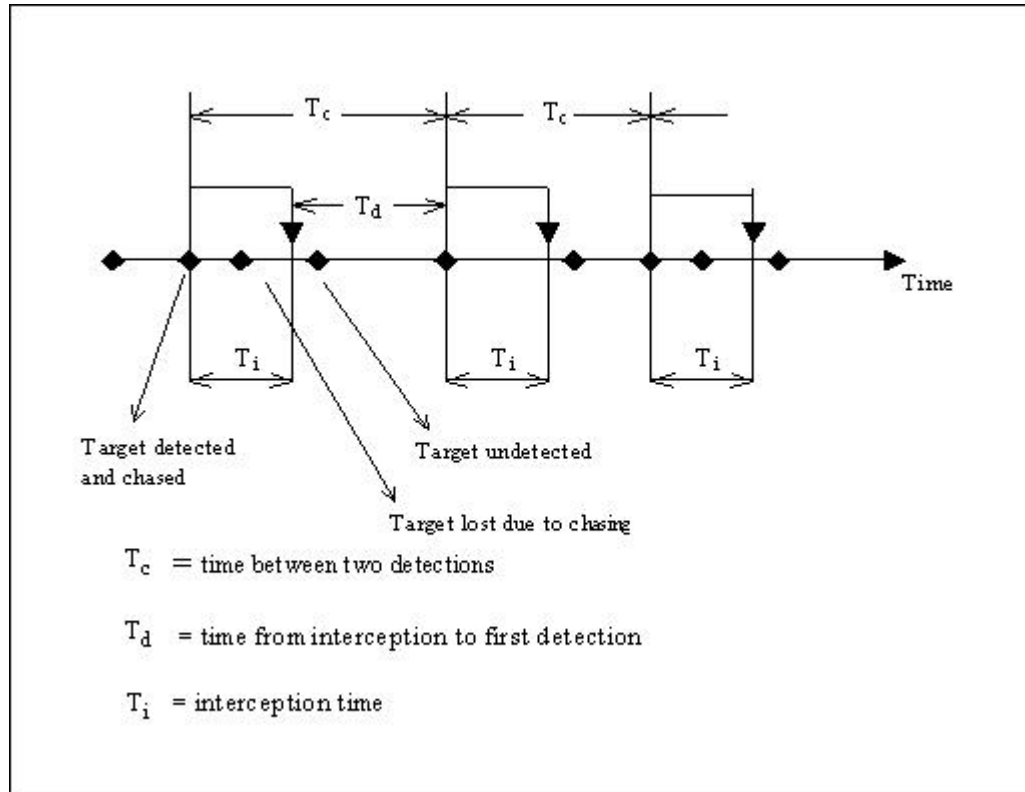


Figure 41. GLI Model

The time between the accomplished interception is the and the next target's detection (T_d) is assumed exponential with mean $\frac{1}{\beta P_d}$ while T_i is the interception time with mean τ , in hours. The probability of detection (P_d) is the computed optimal CDP for the elected search profile.

Let $N(t)$ be the number of intercepted targets to occur during $(0,t]$. $N(t)$ is a renewal counting process (possible delayed) with t assuming values greater than or equal to 0. The following definitions and equations are derived from this process:

- Expected cycle length $E[T_c]$:

$$E[T_c] = E[T_i] + E[T_d] = \tau + \frac{1}{\beta P_d}; \quad (5.5)$$

- Long run average number of targets intercepted per hour (L_{TI}):

$$L_{TI} = \lim_{t \rightarrow \infty} \frac{N(t)}{t} = \frac{1}{E[T_c]} = \frac{\beta P_d}{\tau \beta P_d + 1} \quad (5.6)$$

- Long run average number of targets lost due to GLI per hour (L_{TLG}):

$$L_{TLG} = \frac{E[T_i] \beta}{E[T_c]} = \frac{\tau \beta}{\tau + \frac{1}{\beta P_d}} \quad (5.7)$$

- Long run average total number of targets lost (lost due GLI + undetected) per hour (L_{TLT}):

$$L_{TLT} = \frac{E[T_i] \beta + (1 - P_d) \beta E[T_d]}{E[T_c]} = \frac{\tau \beta + \frac{(1 - P_d)}{P_d}}{\tau + \frac{1}{\beta P_d}} \quad (5.8)$$

The Equations 5.5 through 5.8 are used to obtain the intended campaign's MOEs. The values for each parameter used in these equations were calculated in previous steps. Therefore, by inserting these values in the last four equations, the first set of measures of performance (MOP) is attained and presented at right-bottom of the CDA output. Figure 42 illustrates an example output for a 72 hour campaign period (C_p).

Expected Crossing Targets		12		
		Base 1	Base 2	Both
Expected Tgts Lost	GLI	1.98	1.68	1.34
	CAP	0.59	0.59	0.59
Expected Tgts	GLI	10.02	10.32	10.66
Detected-Chased	CAP	11.41	11.41	11.41
Percentage Interceptable Tgts		0.45	0.52	0.62

Figure 42. Campaign MOPs

The term “Expected Crossing Targets” refers to the total number of targets expected to cross the searched area $E[C_i]$. Since a Poisson process is assumed for this

situation, $E[C_t]$ is equal to the campaign's period (C_p) multiplied by the targets arrival rate β [11,12] as in Equation 5.9:

$$E[C_t] = C_p \beta \quad (5.9)$$

The term "Expected Tgts Lost" refers to the expected total number of targets lost in the campaign's period, and it is divided into two branches according to the interception procedure adopted in the campaign, CAP or GLI. As noticed, there are three columns in this table. The first, Base 1, includes the results when only Air Base 1 is used in GLI procedure. The second column is analogous using Air Base 2, and the last column; "Both" includes the results when both Air Bases are used in the GLI procedure. In this case, the computations are based on the minimum interception time between the two Air Bases. Therefore, an optimal interceptor's utilization is assumed in this situation, that is, the interceptor launched in the mission is always the one in a better position to intercept the target in shorter time.

The term "Expected Tgts Detected-Chased" refers to the expected total number of targets detected in the campaign and is divided into two branches according to the interception procedure adopted in the campaign, CAP or GLI.

The last MOP, percentage of targets intercepted before the preset interception line is related to the preset interception line and its implications. The percentage of targets intercepted before the possible lost is calculated by comparing the GLI procedure time and the time spent by the target from its detection until it reaches the preset interception line (Figure 43). Therefore, the Air Base position will play an important role in the campaign result. The CDA user's interface shows this MOE related to each Air Base as well as a combined result in case of a simultaneous and optimum utilization of two Air Bases (Figure 42).

Base Depth	Int line depth	Target's Time to Preset Line							
		TRUE	TRUE	TRUE	TRUE	TRUE	TRUE	TRUE	TRUE
10	10	10	20	30	40	50	60	70	80
340	290	1.91	1.91	1.91	1.91	1.91	1.91	1.91	1.91
330	280	1.84	1.84	1.84	1.84	1.84	1.84	1.84	1.84
320	270	1.78	1.78	1.78	1.78	1.78	1.78	1.78	1.78
310	260	1.71	1.71	1.71	1.71	1.71	1.71	1.71	1.71
300	250	1.64	1.64	1.64	1.64	1.64	1.64	1.64	1.64
290	240	1.58	1.58	1.58	1.58	1.58	1.58	1.58	1.58
280	230	1.51	1.51	1.51	1.51	1.51	1.51	1.51	1.51
270	220	1.45	1.45	1.45	1.45	1.45	1.45	1.45	1.45
260	210	1.38	1.38	1.38	1.38	1.38	1.38	1.38	1.38
250	200	1.32	1.32	1.32	1.32	1.32	1.32	1.32	1.32
240	190	1.25	1.25	1.25	1.25	1.25	1.25	1.25	1.25
230	180	1.18	1.18	1.18	1.18	1.18	1.18	1.18	1.18
220	170	1.12	1.12	1.12	1.12	1.12	1.12	1.12	1.12
210	160	1.05	1.05	1.05	1.05	1.05	1.05	1.05	1.05
200	150	0.99	0.99	0.99	0.99	0.99	0.99	0.99	0.99
190	140	0.92	0.92	0.92	0.92	0.92	0.92	0.92	0.92
180	130	0.86	0.86	0.86	0.86	0.86	0.86	0.86	0.86
170	120	0.79	0.79	0.79	0.79	0.79	0.79	0.79	0.79
160	110	0.72	0.72	0.72	0.72	0.72	0.72	0.72	0.72
150	100	0.66	0.66	0.66	0.66	0.66	0.66	0.66	0.66
140	90	0.59	0.59	0.59	0.59	0.59	0.59	0.59	0.59
130	80	0.53	0.53	0.53	0.53	0.53	0.53	0.53	0.53

Figure 43. Target's Flight Time To Preset Interception Line

D. SUMMARY

This chapter presented the final product of this thesis: the campaign decision aid. This tool was a consequence of the integration of several technical and operational parameters of the R-99, the optimized patrolling profile selection, and the other air defense assets involved in the scenario proposed in Chapter II. Besides this computerized integration, the CDA generates some measures of performance that are very useful to evaluate the overall campaign effectiveness. Its automated characteristic allows to the decision-maker an immediately response about the main aspects involved in campaigns. Therefore, the CDA flexibility possibilities a quantifiable comparison of the alternatives to the mission execution, as Air Base selection, interceptor aircraft needs, interception tactics, in terms of expected effectiveness results. Another important by-product of the CDA is the possibility of estimating the campaign's cost and manpower required to conduct the overall operation.

THIS PAGE INTENTIONALLY LEFT BLANK

VI. CONCLUSIONS AND RECOMMENDATIONS

A. GENERAL

Recently, the Brazilian Air Force was equipped with a new Airborne and Control System (AWACS), the R-99. This Brazilian made aircraft is intended to establish an effective surveillance in the Amazonian region. This region has been frequently crossed by illicit air traffic, normally related to narcotics transportation. Furthermore, this region has been the focus of recent media reports about revolutionary foreign forces trying to expand their influence across the Brazilian border. This thesis investigates R-99 employment options for maximizing mission effectiveness with limited assets. Since the area for possible illicit air traffic is extensive, this thesis develops of a tactical planning tool for optimum employment of the R-99 in these campaigns.

To start the development of this planning tool, a specific scenario where the R-99 will operate is defined. The scenario incorporates some assumptions necessary to scope the thesis as well as to meet the requirements for Search and Detection Theory's application.

The thesis then exploits Radar Theory to select the factors related to a typical patrolling mission. In addition, Radar Theory is used to obtain the unavailable data required to analyze and evaluate the R-99's flight patrolling profiles. The detailed aircraft technical and operational data collected in this phase is used to set up the lateral range function. In this function elaboration, the profile dynamics (searcher and target relative movements) are used to define the proper sensor sweep width for a specific patrolling geometry.

Two feasible patrolling geometries or profiles are analyzed: symmetric linear and symmetric crossover. Each of these profiles was separately analyzed and evaluated in terms of probability of detection effectiveness. All influential parameters for each profile are listed, evaluated, and related to its specific contribution in the overall profile result. The results were then compared and the significant findings were explained. This initial

methodology only evaluated the R-99 surveillance capability for different patrolling profiles.

In order to integrate the R-99 detection capabilities and target interception task, Air Base locations and their influence in terms of search time availability (on station time) were analyzed in relation to the patrolling profiles. The location of the Bases is also related to the ground launch interception effectiveness when compared to the combat air patrol (CAP) interception tactic. To avoid specific calculations for each factor mentioned in this integration procedure a computerized campaign decision aid was developed. The campaign decision aid incorporates all influential parameters investigated in this thesis and enables the user to obtain an immediate evaluation of the potential campaign's effectiveness for the different tactical factors enumerated.

In this function elaboration, the profile dynamics (searcher and target relative movements) are used to define the proper sensor sweep width for a specific patrolling geometry.

Two feasible patrolling geometries or profiles are analyzed: symmetric linear and symmetric crossover. Each of these profiles was separately analyzed and evaluated in terms of probability of detection effectiveness. All influential parameters for each profile are listed, evaluated, and related to its specific contribution in the overall profile result. The results were then compared and the significant findings were explained. This initial methodology only evaluated the R-99 surveillance capability for different patrolling profiles.

In order to integrate the R-99 detection capabilities and target interception task, Air Base locations and their influence in terms of search time availability (on station time) were analyzed in relation to the patrolling profiles. The location of the Bases is also related to the ground launch interception effectiveness when compared to the combat air patrol (CAP) interception tactic. To avoid specific calculations for each factor mentioned in this integration procedure a computerized campaign decision aid was developed. The campaign decision aid incorporates all influential parameters investigated in this thesis

and enables the user to obtain an immediate evaluation of the potential campaign's effectiveness for the different tactical factors enumerated.

B. CONCLUSIONS

Throughout this thesis, many significant operational findings were identified. Some are related to the R-99's detection capabilities while others are associated with overall campaign integration. The following is a list of specific conclusions identified during the analysis and evaluation of the R-99 surveillance capabilities, patrolling profiles particularities, and campaign effectiveness.

1. R-99 Surveillance Capabilities

Due to the Erieye antenna characteristics, vertical and horizontal radar silence zones occur around the R-99. The effects of this radar restriction are summarized below.

The vertical radar silence zone is associated with the 3 dB beamwidth, the minimum detection range and the platform flight altitude. The lower the platform is, the smaller the vertical radar silence zone is. However, lower flight altitudes also reduce the radar horizon, causing reduction in the overall radar coverage at lower altitude levels. Therefore, an optimal altitude in terms of radar ground coverage is a trade off between the vertical radar silence zone and the radar horizon, when considering the limitations about minimum and maximum range detection. To achieve the best range coverage for detecting targets flying at 500 ft., the optimal altitude for the R-99 was 5775 ft. Higher or lower R-99 flight altitudes resulted in smaller radar coverage ranges.

The horizontal radar silence zone is associated with the antenna electronic scanning, minimum and maximum detection ranges as well as the platform altitude. The minimum detection range produces a detection inner gap, which causes the low level target's detection to vary conversely to the platform altitude. The antenna's electronic scanning produces silence radar angles near the aircraft fuselage so that the detection zone is concentrated on the area perpendicular to the longitudinal aircraft axis. When analyzed statically, a significant detection limitation at the rear and at the front aircraft's position exists. However, when analyzed dynamically, this restriction is reduced because

the relative target-searcher approaching angle. The combination of target and searcher vectors can be used to avoid the horizontal radar silent zone. Therefore, this vector dynamics has to be considered when analyzing the radar sweep width. The reason for this is because its calculation includes the lateral range function, which varies according this vector dynamics. The dynamics are different for each of the two profiles analyzed in this thesis, and their effects on each of these profiles are detailed below.

2. Patrolling Profiles Particularities

a. Searcher and Target Speed Effects

The vector dynamics previously mentioned affect the sweep width of both patrolling profiles. In both cases the radar sweep width is reduced or increased by increasing or reducing the searcher speeds respectively, assuming a constant target speed. Although augmenting the searcher speed causes the sweep width to decrease in both patrolling profiles, the cumulative detection probability (CDP) still increases. Therefore, greater searcher speeds always result in better CDP independent of patrolling profile or target speed.

Although search speed improves CDP in both profiles, this effect is more evident in the crossover patrolling geometry. Given a particular target speed, the linear profile varies the CDP by 20%. However, for the same searcher speed variation, using a crossover profile, the CDP varies 100%. Another effect related to searcher speed is that for a given target speed, the linear profile achieves better CDPs at lower range searcher speeds. At higher searcher speeds the crossover profile becomes a better option in terms of CDP results.

b. Searcher Altitude Effects

An important difference between the two patrolling profiles is the altitude effects on CDP. While the linear profile is not affected by altitude, the crossover profile presents CDP variations above and below the optimal coverage altitude. For the altitudes above the optimal coverage altitude, the higher the searcher, the lower the CDP.

The combination of speed and altitude effects on CDP for each patrolling profiles are summarized in the following way: when the time on station is not required to be large, the crossover profile is a better option. This results in more fuel availability, which allows profiles with higher speeds and low altitudes. The opposite relationship holds for the linear profile.

3. Campaign Effectiveness

Campaign effectiveness may be measured in terms of number of targets intercepted during the operation. This result depends on various factors such as:

- The number of available Air Bases as well as their relative position to the searched area
- The searched area's length, the interceptors' speed, the position where the target is detected
- The patrolling profile, the preset interception line, the interception tactics (GLI or CAP)
- The inter-target time
- The target speed

As observed, the variables involved in this measurement are numerous. Some of these variables may assume a wide range of possibilities, such as interceptor speed or interception tactics. Other variables may not, as in the case of the Base's location and area searched. Therefore, each case has to be evaluated for the intended campaign and their respective particularities. Nonetheless, some conclusions were identified through this thesis and are enumerated in the following paragraphs.

a. Interceptor Speed

The faster the interceptor, the higher the number of detected targets and the higher the percentage of targets intercepted. This comment is applicable to both interceptor procedures (GLI or CAP); however, the effects are more evident when GLI is the chosen tactic.

b. Interception Tactics

The combat air patrol (CAP) interception is always better than the ground launch interception (GLI) since the MOE results in better outcomes. That is, the expected number of targets lost is smaller, the number of targets detected is higher, and the number of targets capable of being intercepted is higher during campaign. However, the logistic support as well as the personnel required to maintain a CAP station during an entire campaign has to be evaluated and compared to the means available for the operation.

c. Preset Interception Line

Moving the preset interception line far from the borderline increases the target flight time more than the interceptor flight time to this line, since the interceptor speed is assumed to be higher than target speed. Therefore the farther the preset interception line is from the borderline; the higher is the percentage of targets capable to be intercepted.

d. Searcher's Base Relative Location

Base location is an important aspect to be considered in the campaign planning. This is because the time spent in transit to and from the search area is subtracted from the available time of flight. As a consequence, the farther a base is relative to the search area restricts the flight profiles (altitudes and speeds) available and negatively affects the CDP. Furthermore, some bases' location may be completely restrictive in terms of mission continuity, so that the number of searchers has to be increased in order to avoid search interruption. Therefore, the closer the base is to the search area, the more flexible the profile selection and required number searchers needed for an uninterrupted campaign.

Although the number of variables needed to be correlated is numerous for MOE evaluation, the Campaign Decision Aid (CDA) provides immediate response to any desired campaign. Besides this prompt calculation, the CDA is very flexible regarding new input data. Radar parameters, R-99 operational data, target altitudes, Air Bases locations, interceptor types are easily changed by the user. Because of this flexibility, the CDA can be used for different AWACS (Airborne Warning and Control System) than the

R-99 and in different scenarios. For these reasons, CDA is also a useful tool in planning and comparing alternative missions.

C. RECOMMENDATIONS

1. Validation of the CDA

The CDA outputs should be validated in a simulated operational exercise. In this operational exercise, target aircraft should have to cross a pre-determined imaginary borderline at speeds corresponding to the underlying probability distribution assumed in this thesis. The scenario for this exercise should be mounted in the Amazon region to achieve as much realism as possible. The duration of the campaign is crucial and should be sufficient to evaluate the results using a renewal process since the scenarios used in this methodology were limited.

2. Radar Performance Testing

Operational Test Evaluation should be conducted to confirm the data derived analytically using Radar Theory and some assumptions about the detection capabilities. The testing should include radar parameters evaluation throughout different R-99 altitudes, R-99 and target speeds, and target radar cross-section. The test should be implemented in the Amazon region to achieve more realism and consequently more reliability to the testing results.

3. Areas For Future Research

Two areas for further research are presented below.

a. R-99 Data Analysis

A comparative analysis of R-99 test data and CDA data should be conducted. The data collection is intended to confirm or improve the data derived analytically using Radar Theory and to feed the models with the proper probability distributions. For the first purpose, Operational Test and Evaluation (OT&E) is the suggested method to conduct this data collection. Ideally, this activity should be

conducted in a region with the same characteristics as those presented in the campaign scenario, which would guarantee more fidelity in the results obtained. Additionally, the R-99 can be evaluated operationally and the deficiencies can be corrected before a real employment. For the second purpose, the data referent for each assumed expected value has to be collected and analyzed. All data analysis tools should be used for this task in order to find out the proper probability distribution for each situation modeled in this thesis.

b. Model Simulation

Model simulation should be conducted to crosscheck the results analytically obtained and to foster some new insight into the geometries and profiles illustrated in this thesis. The data collected and evaluated during testing should be used as a basis for the simulation

The feedback collected from both testing and simulation is very important for the improvement of the CDA, that is, model-test-model is a key methodology for a reliable application of the CDA.

LIST OF REFERENCES

1. Skolnik, Merrill Ivan. *Introduction to Radar System*, McGraw-Hill, 1980.
2. Chudnovsky, David V. and Chudovsky, Gregory V., *Search Theory- Some Recent Developments*, Marcel Dekker, Inc., 1989.
3. Haley, Brian K. and Stone, Lawrence D., *Search Theory and Applications*, Plenum Press, 1980.
4. Lawrence D., *Theory of Optimal Search*, Academic Press, Inc. (London) Ltd, 1975.
5. Ericsson Microwave Systems AB. *Erieye Radar - Technical Data*. Estocolmo, 1998
6. Washburn, Alan R., *Search and Detection*, Military Applications Section Operations Research Society of America c/o Ketron, May 1981.
7. Long, Maurice W., *Airborne Early Warning System Concepts*, Artech House, Inc., 1992.
8. Moris, G. and Harkness, L., *Airborne Pulsed Doppler Radar*, Artech House, Inc., 1996.
9. Streetly, Martin, *Jane's Radar and Electronic Warfare Systems*, 14th edition, 2002-2003.

10. Wagner, Daniel H., Mylander C. and Sanders, Thomas J., *Naval Operations Analysis*, Naval Institute Press, 1999.
11. Gaver, Donald. P., Jacobs, Patricia A. and Stoneman, J, *Analytical Models for Mobile Sensor (UAV) Coverage of a Region*, Operations Research Department, Naval Post-Graduate School, 1999.
12. Ross, Sheldon M., *Introduction to Probability Models*, Department of Industrial Engineering and Operations Research, University of California, 7th edition, Academic Press, 2000.
13. Jacobs, Patricia A., *Class Notes for OA 4301*, Operations Research Department, Naval Post-Graduate School, 2002.
14. Hetzler, John C. Jr., *The Application of Operations Analysis to Weapons Systems Developments*, United States Naval Ordnance Laboratory, White Oak, Mariland, 5 Aug 1969.

INITIAL DISTRIBUTION LIST

1. Defense Technical Information Center
Ft. Belvoir, Virginia
2. Dudley Knox Library
Naval Postgraduate School
Monterey, California
3. Comando Geral do Ar
Comando da Aeronautica, Ed. Anexo
Esplanada dos Ministérios
Brasília, DF, 70064-901, Brazil
4. COL Narcélio Ramos Ribeiro
CGEGAR / COMGAR
Comando da Aeronautica, Ed. Anexo
Esplanada dos Ministérios
Brasília, DF, 70064-901, Brazil
5. Dr. José Edimar Barbosa
Instituto Tecnológico da Aeronáutica - ITA
Praça Marechal Eduardo Gomes, 50
Divisão de Engenharia Eletrônica - IEE
São José dos Campos, SP, 12229-900, Brazil
6. Dr. Steven E. Pilnick
Department of Operations Research
Naval Postgraduate School
Monterey, CA 93940